Accepted Manuscript

The cell in the ink: Improving biofabrication by printing stem cells for skeletal regenerative medicine

G. Cidonio, M. Glinka, J.I. Dawson, R.O.C. Oreffo

PII: S0142-9612(19)30220-0

DOI: https://doi.org/10.1016/j.biomaterials.2019.04.009

Reference: JBMT 19164

To appear in: *Biomaterials*

Received Date: 26 November 2018

Revised Date: 28 March 2019

Accepted Date: 6 April 2019

Please cite this article as: Cidonio G, Glinka M, Dawson JI, Oreffo ROC, The cell in the ink: Improving biofabrication by printing stem cells for skeletal regenerative medicine, *Biomaterials* (2019), doi: https://doi.org/10.1016/j.biomaterials.2019.04.009.

The cell in the ink: improving biofabrication by printing stem cells for skeletal regenerative medicine

G. Cidonio[1,2], M. Glinka[1], J. I. Dawson[1], R.O.C. Oreffo[1*]

[1]Bone and Joint Research Group, Centre for Human Development, Stem Cells and Regeneration, Institute of Developmental Sciences, University of Southampton, Southampton, UK

[2]Engineering Materials Research Group, Faculty of Engineering and the Environment, University of Southampton, Southampton, UK

*Corresponding author. Tel.: +44 (0)23 81 208502, fax: +44 (0)23 81 205255

Email address: richard.oreffo@soton.ac.uk

Keywords: cell printing, bioink, biofabrication, bioprinting, hydrogels, additive manufacturing, 3D printing

Abstract

Recent advances in regenerative medicine have confirmed the potential to manufacture viable and effective tissue engineering 3D constructs comprising living cells for tissue repair and augmentation. Cell printing has shown promising potential in cell patterning in a number of studies enabling stem cells to be precisely deposited as a blueprint for tissue regeneration guidance. Such manufacturing techniques, however, face a number of challenges including; (i) post-printing cell damage, (ii) proliferation impairment and, (iii) poor or excessive final cell density deposition. The use of hydrogels offer one approach to address these issues given the ability to tune these biomaterials and subsequent application as vectors capable of delivering cell populations and as extrusion pastes. While stem cell-laden hydrogel 3D constructs have been widely established *in vitro*, clinical relevance, evidenced by *in vivo* long-term efficacy and clinical application, remains to be demonstrated. This review explores the central features of cell printing, cell-hydrogel properties and cell-biomaterial interactions together with the current advances and challenges in stem cell printing. A key focus is the translational hurdles to clinical application and how *in vivo* research can reshape and inform cell printing applications for an ageing population.

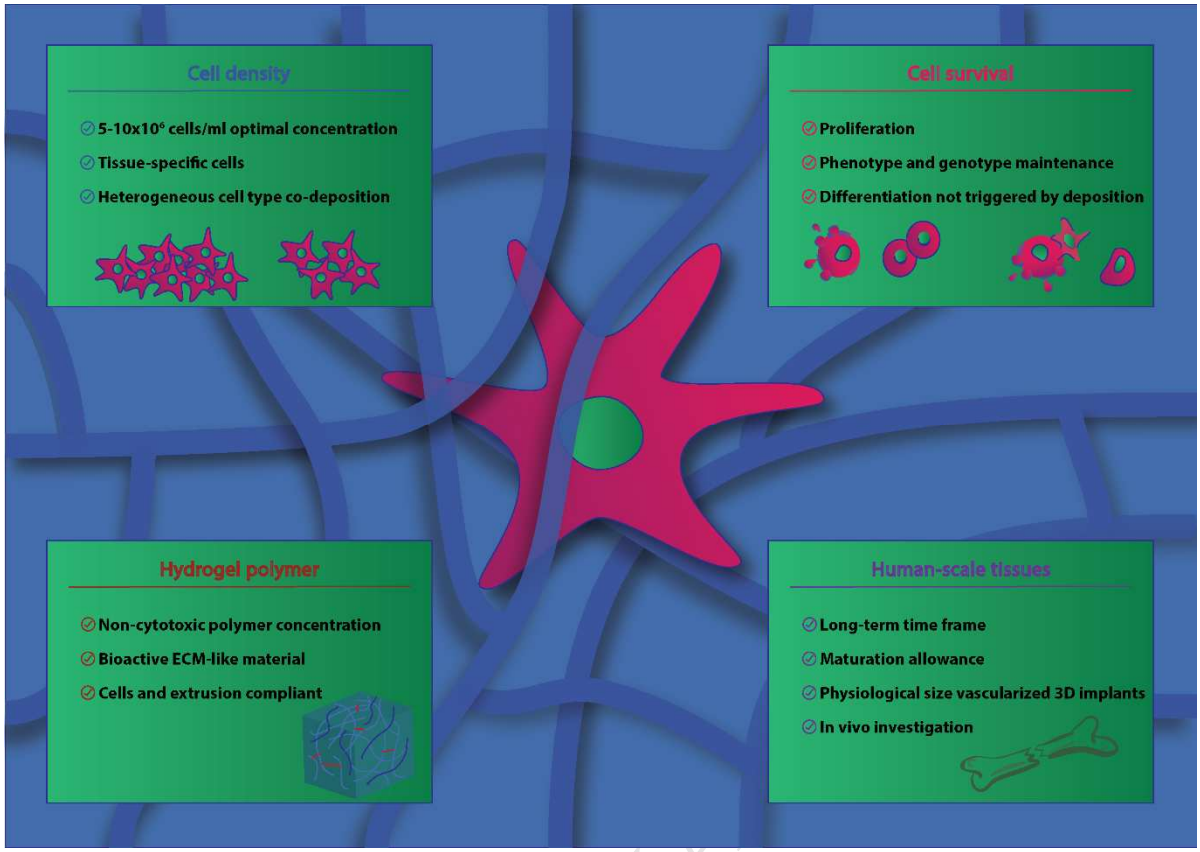

Graphical Abstract

Cell printing - capacity and limitations. Cell type and density are important factors in the printing of living cells. Post-printing consequences including: (i) impaired cell proliferation, (ii) maintenance of phenotype and genotype, (iii) preservation of cell integrity and morphology are issues that need to be considered. Stem cell printing aims to deposit cells in three dimensions within an environment conducive to proliferation and differentiation. Therefore, long-term investigations of cell viability and proliferation *in vitro* and *in vivo* are required to elucidate construct maturation and effective tissue regeneration and integration. Importantly, the properties of the hydrogel cell carrier (biocompatibility, bioactivity, physical characteristics) for the select 3D print approach envisaged are crucial for cell encapsulation, protection and support during differentiation and proliferation.

1. Introduction

Cell printing offers significant promise as an engineering technology to orchestrate tissue and organ regeneration including application, at scale, for human tissue formation and reparation [1]. Since the early seminal studies using cell deposition (cytoscribing) with a common desktop inkjet printer [2], major advances have been achieved in the arena of cell printing. Cell printing intends to position gel-like materials loaded with living cells (referred to as bioink) in a layer-by-layer fashion through an automated dispensing system. The attraction lies in the ability to apply this tissue engineering (TE) technology to generate readily implantable, tissue-relevant, 3D structures [3] to enhance the reparative processes.

In contrast to the use of standard cell seeding approaches, cell printing technologies incorporate cells within 3D implants to provide an improved biomimetic cell/material arrangement. Currently, two-dimensional monolayer cell culture remains the conventional platform for cell expansion and *in vitro* investigations. However, cells are naturally able to sense their surrounding three-dimensional environment resulting in adaptations to growth and differentiation [4]. To address these limitations, cell printing technologies have come to the fore, through the application of computer-based motion controls and biomaterial cell-carriers to fabricate 3D bioconstructs. These cell-laden scaffolds can recapitulate the 3D cell-niche environment including spatially organized homing signals essentials for tissue regeneration purposes.

This innovative tissue engineering technology, whilst widely accepted, presents a number of challenges to *in vivo* efficacy for tissue fabrication. These include:

i) the requirement for biomaterials used for cell printing to mimic specific tissue extracellular matrix (ECM) physical and chemical properties,
ii) the requirement for viscoelastic properties to allow both post-printing stability and appropriate fluidity for cell protection within the printing nozzle [5,6], and
iii) the ability to preserve the viability of embedded cells during printing and host functional viable cells post-printing until remodelling and regeneration is complete.

This review will focus on recent research on 3D printing and in particular the challenges associated with printing living cells to generate viable and functional three-dimensional tissue constructs. We will describe the use of various biomaterials commonly applied for cell printing and their limitations with a particular focus on those of promise for skeletal regeneration. Finally, we discuss the current challenges in cell printing for engineer living tissues, listing relevant studies on how cell density, shear stress, printing parameters, nozzle shape and crosslinking, can affect post-printing viability and functionality. We will highlight, in particular, current advances and challenges in skeletal stem cell printing including the translational hurdles that need to be overcome to ensure clinical application and how *in vivo* research can reshape and inform cell printing for therapeutic application.

2. Cell Printing: State-of-the-Art

Cell printing is developing apace with input and innovation from a range of disciplines including engineering, physics, materials chemistry and biology. Developments include the novel use of 3D printing technology incorporating bacteria in a hydrogel to generate a “functional living ink” that can impact in bioremediation (e.g. phenol waste removal) and biomedical (e.g. in situ biomaterial production) applications [7]. Tissue engineering application of cell printing are many but typically, focus on the manufacture of cell-laden 3D constructs to resemble the geometry and complexity of human tissues. Harnessing the biofabrication rationale (Fig. 1), cells are isolated from donor tissue, encapsulated within cytocompatible polymeric matrices and printed at a resolution that matches the heterogenic components of natural tissue in the 10-100 µm range [8].

Hydrogels are highly hydrated polymeric matrices [9] commonly used as biomaterial inks for 3D bioprinting. Three-dimensional hydrogel matrices (Fig. 2) can function as an injury site ECM scaffold for stem cell-mediated tissue-regeneration, or to deliver bioactive molecules to promote endogenous progenitor cell migration and differentiation [10]. Hydrogels have been engineered for application as cell carriers for a plethora of cell printing systems. In the following sections we describe the key cell printing technologies in current use, including inkjet printing followed by laser [11] and extrusion-based bioprinting [12,13], and characterise a number of hydrogels that can be utilised as structural support for cells.

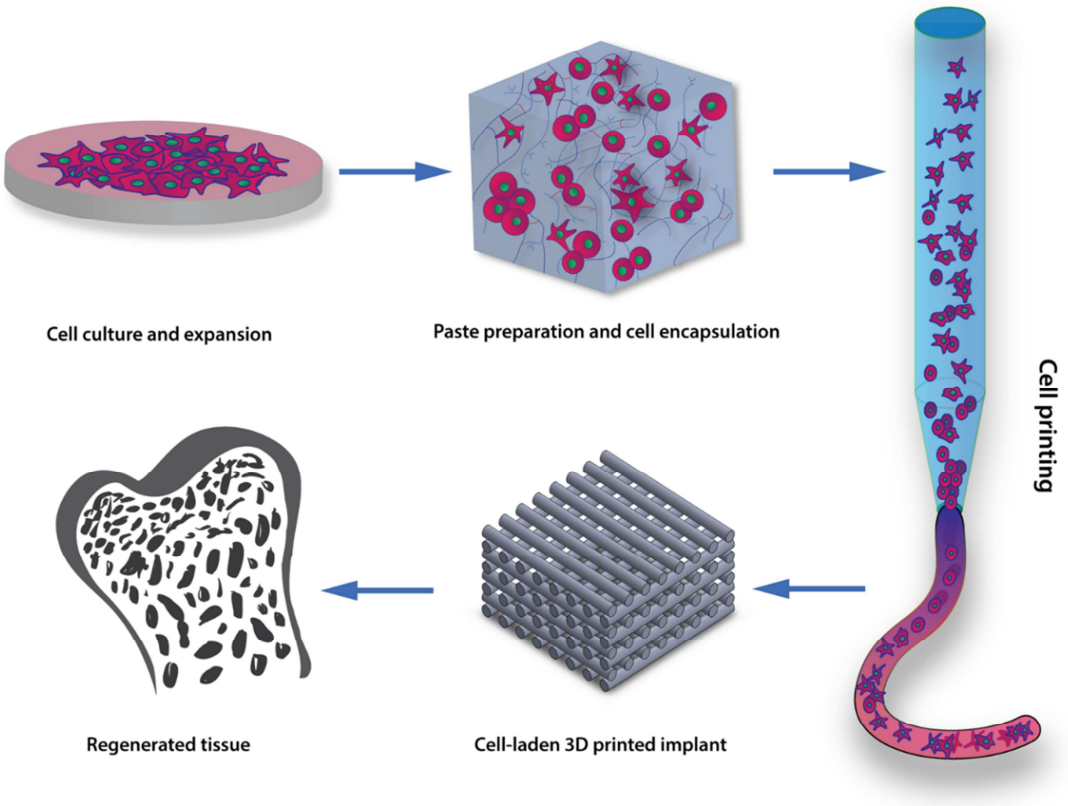

Fig. 1. The cell printing paradigm. Cell printing involves cell incorporation or encapsulation within biomaterials possessing viscoelastic properties that allow their use as a “bioink”. Upon printing, cell-laden 3D printed

structures are fabricated with the aim, ultimately, of implantation into the patient to regenerate the specific tissue of interest.

2.1 Inkjet Bioprinting

Inkjet-based bioprinting, first developed by Thomas Boland (Clemson University) in 2003 [14,15], is a widely employed, low cost, high speed 3D printing technology. 3D inkjet printing platforms were first optimized for generating 3D constructs from a commercial 2D ink-based desktop printer in 2008 [14–17]. Liquid state hydrogels were deposited as a defined spot using thermal-, acoustic- or electromagnetic-induced physical displacement. The volume of the droplet can vary between 1-100 pl which equals to 1-30 µm in size [18]. The thermal or mechanical stresses employed for extrusion purposes represent a considerable disadvantage for this type of printer with cell density and cell death during printing significant limitations. Droplets low in cell percentage can be controlled with high efficiency and thus, to some extent, reduce shear stress and machine nozzle blockage. However, low cell density affects viability and, importantly, the tissue formation capability of the constructs. Modern inkjet printers are able to handle hydrogels in their liquid state with low viscosity given their droplet/jet physical formation.

In a recent study, Gao *et al.* printed human mesenchymal stromal cells (MSCs) in a layer-by-layer fashion [19,20]. Thus, poly(ethylene glycol) alone [20] or dimethacrylate - gelatin methacrylate (PEG-GelMA) [19] mixed with MSCs were printed into a cylindrical construct and cultured for up to 21 days stimulating early differentiation into bone and cartilage resembling tissues. Difficulties in the specific selection of bioink viscosity were reduced by modifying the mechanical properties of materials such as PEG-GelMA. In this way, the authors printed cell-laden scaffolds to achieve an improved uniform distribution of MSCs within a deposited matrix in contrast to non-printed PEG-GelMA scaffolds. While low viscosity ensures good cell viability during printing, this presents challenges for shape fidelity. A recent approach applied combinations of several highly printable bioinks (e.g. alginate-pluronic PE6800, alginate-PEG) using permanent and sacrificial ink to optimise the printing of complex shape constructs [21]. The multi-head inkjet printing system in this case was able to deposit multiple materials, and by the inclusion of muscle progenitor cells in the sacrificial ink, to produce a perfusable 3D *in vitro* model. An alternative approach to improving shape fidelity of low viscosity inks is to harness rapid gelation properties upon deposition. For example, Hedegaard *et al.* [22] used inkjet printing to deposit peptide amphiphiles (PAs) which, in protein-rich solutions, display instantaneous self-assembly to generate complex microstructures which could be modulated by tuning the inkjet propulsion, the impact speed and the bath solutions.

Although versatile and easy-to-use, inkjet cell printing technology is still, to date, not applicable to the development of human-size bioconstructs given issues with droplet non-uniformity, poor cell density, frequent nozzle blockage and physical stresses on cells (e.g. thermal and frequency shocks).

2.2 Laser Bioprinting

Laser bioprinting [23–27] is an effective process in preserving high cell viability following cell-deposition. This nozzle-free technique is based on laser-induced forward transfer (LIFT)

physics through which cells seeded on a donor slide (covered in a radiation absorbing layer) can be safely propelled, encapsulated within droplets of biomaterial, toward a collector slide. The bioconstruct droplet resolution is influenced by the biomaterial rheological properties, donor-collector system, laser energy and resolving power. Laser bioprinting approaches require specific biomaterials with defined viscoelastic properties to ensure that the biomaterial/cells constructs can rapidly gelate to ensure high-defined shape retention [26].
LIFT-based bioprinting have been reported to offer the most useful approach for two-dimensional patterning of cells, yet a few recent studies have shown the potential to produce complex 3D patterns using this approach. Xiong *et al.* [24] applied matrix-assisted pulsed-laser evaporation direct-write (MAPLE DW) approaches to print 3D alginate-fibroblast hollow tubes. Despite the development of such a printing approach to enable a highly accurate and detailed 3D construct, the resultant printing process was slow. In addition, cell viability, noted to be 63.8% immediately upon printing was observed to be 68.2% after 24 h. Low cell survival rate could be caused by both cell injury upon printing (mechanical stress during droplet/jet formation and landing) and the requisite stationary conditions (45 min) to allow gel crosslinking. Using a similar approach, Gruene *et al.* [23] successfully generated a MSCs graft using LIFT technology with evidence of chondrogenic and osteogenic differentiation evidenced by osteocalcin (OC) and alkaline phosphatase (ALP) activity. Hence, stem cells were able to survive the print process and retain their osteogenic differentiation capacity.
Technologies such as stereolithography (SLA) or digital light processing (DLP) are reliable alternatives to LIFT for producing viable cell-laden constructs. SLA and DLP systems utilise the photopolymeric properties of the material (or compounds mixed with it) to solidify the liquid and thus form a 3D construct. The curing process is commonly carried out simultaneous with the printing via exposure to ultraviolet (UV) [28] or visible light [29]. Recently, Lim *et al.* [29] have employed methacrylated poly(vinyl alcohol) (PVA-MA) and gelatin (Gel-MA) to fabricate cell-laden constructs via direct visible light processing proving the high resolution (25 μm) printing platform is suitable for producing viable and functional cell-laden constructs

At present, laser-based techniques offer the possibility to print cells with low damage, although, critically, require (i) specific bioink gelation properties for application, (ii) expensive fabrication costs and, (iii) a skilled workforce to operate the platform technology.

2.3 Extrusion-Based Bioprinting

Extrusion-based bioprinting is a widely used rapid prototyping approach, able to deposit precisely hydrogels with shape retention depending on the physical and chemical properties of the biopolymer used. Extrusion-based bioprinting is currently one of the most widely employed platforms for cell printing given the advantages of ease of handling, ability to customise and versatility of the systems available [30–32]. Extrusion-based bioprinting typically uses post-processing or temperature-sensitive hydrogels for cell delivery. Post-printing processes (e.g. cross-linking, UV-curing, etc.) are widely employed for altering physio-chemical gel properties accelerating gelation phenomenon, strengthening the overall matrix structure and for tuning polymeric degradation. The use of specific hydrogels as cell carriers can highly influence cell viability after printing. Fedorovich *et al.* [33] investigated the differentiation potential of MSCs within organised cell-laden constructs. Cells were included within different types of hydrogels such as synthetic Lutrol F127 (PF127), matrigel, alginate

and agarose. Lutrol and agarose extrusion resulted in precise deposition with a 150 µm nozzle tip, however with limited cell survival following printing in comparison to matrigel and alginate, emphasising the influence of material choice in the cell printing process. Cells can be encapsulated in modified-composite bioinks that enable shape fidelity post-printing even at low polymeric concentrations, preserving cell viability and sustaining proliferation. We have recently [31] demonstrated the ability of a novel clay-based hydrogel to encapsulate human skeletal stem cells and to generate high resolution cell-laden 3D scaffolds. The nanocomposite bioink was developed using a nanosilicate suspension blended with alginate and methylcellulose to ameliorate shear thinning properties, shape fidelity, mechanical stability and growth factor localisation. Following extrusion, 70-75 % of the printed cells survived the process, showing augmented proliferation rate compared to the control group (clay-free). This low-polymer content bioink facilitated cell printing, retaining viability after printing and supported cell proliferation over 21 days of culture.

Extrusion-based cell printing remains a popular approach given the wide versatility available in the system but, remains limited in resolution [34–36]. Cell printing, based on extrusion techniques, represent an exciting approach for organ printing given, i) the plethora and diversity of compatible materials that can be used, ii) the potential for cell inclusion and, iii) parameter variation available as a consequence of further modulation of printer parameters and scalability.

3. Hydrogels for Cell Printing

3D printed scaffolds for tissue regeneration purposes can involve biomaterials alone (*cell-free*), cells alone (*scaffold-free*) or a combination of the two (*cell-laden*). The majority of biomaterials used in cell printing approaches are hydrogels. The high water content of hydrogels can also promote nutrient diffusion and waste removal, while, manipulation of hydrogel properties can enable the rapid or prolonged released of a drug or molecule of interest [10,37]. To be employed as a cell-encapsulation vector for 3D printing applications, hydrogels should present specific rheological and gelation properties tuned according to the 3D fabrication process. The ultimate purpose for such polymeric matrices is to direct and guide tissue-specific cell lineage formation and to maintain cell proliferation and phenotype [38].

3.1 Cell-Free, Scaffold-Free and Cell-Laden Hydrogel Printing

Cell-free (acellular) biomaterial deposition processes, with further post-printing cell addition, remain the most common bioprinting techniques in use. Although printing viscous hydrogels can enable the fine deposition of the material with subsequent cell-seeding, results from acellular approaches are far from ideal. The acellular approaches may lack the requisite functionality critical for *in vivo* regeneration. Nevertheless, acellular implants are frequently used in the clinic for bone repair. Recently, Reznikov *et al.* [39] used a 3D printing approach to generate acellular 3D scaffolds incorporating a stiffness gradient which was able to modulate the response of endogenous progenitor cells in a large animal defect model (Fig. 3 *Acellular*). Acellular implants have been reported to show substantial tissue ingrowth

in vivo but with a lower degree of ECM organization compared to cell-laden 3D hydrogel implants [40]. It is important to note, post-printing seeding approaches cannot ensure the requisite cell density, cell spreading, attachment, migration and interaction both *in vitro* and *in vivo*. Acellular 3D printed constructs thus have limited capacity for cell homing, restricting space available for post-seeded cells. Nevertheless, hydrogel coating [41] or hydrogel-mediated cell seeding [42] could represent a promising approach especially in hard tissue regeneration applications. For example, 3D printed cell-free ceramic such as β-tri-calcium phosphate (β-TCP) can be perfused with softer cell-laden hydrogels for effective cell delivery and encapsulation [9,43].

Scaffold-free approaches have come to the fore, as promising manufacturing techniques, to engineer 3D constructs using, exclusively, living cells and the absence of any support or encapsulating biomaterial [23,44–46]. For example, Arai *et al.* [46] recently fabricated a scaffold-free tubular cardiac implant and proved the efficacy of this construct as a cardiac pump. (Fig. 3 *scaffold-free*). Cardiac spheroids were run through an array of fine needles using a computer-controlled robotic arm. Spheroid fusion and the contraction of the three-dimensional construct implied the potential functionality of this construct. Taniguchi *et al.* [45] used an unconventional Regenova bioprinter to build a fully functional tracheal substitute via Cyfuse's method. In a similar approach to Arai *et al.* [46] functional multi-cellular organoids (chondrocytes, endothelial cells and mesenchymal stem cells) have also been deposited and fused into a tubular shape. The results of this organoid printing approach, though promising when constructs were implanted *in vivo,* raised questions of practical feasibility. Issues included: i) the high number of spheroids required (384 spheroids for 5 mm long construct), ii) poor structural integrity (artificial trachea resulted significantly less strong than 8-week old rat trachea) and, iii) the long timescale required for full implant maturation (28 days).

Cell-laden printing approaches can manufacture biomimetic human-like tissues with stem cells encapsulated in biomaterials able to initiate and stimulate new tissue ingrowth acting as primitive building blocks (Fig. 3 *cell-laden*) [30,31,33]. The cell-carrier hydrogels are typically doped with GFs, bioactive compounds or macromolecules to aid cell metabolism [9,47]. The hydrogel design should therefore consider both cell microenvironment and printing capabilities. High printing accuracy can be achieved due to tuned gel viscosity reducing strand failure. Nevertheless, the selected biomaterial for cell encapsulation should retain the capacity to be extruded with minimum applied shear force to avoid cell damage and reduce cell viability [48,49]. Biomaterials commonly used in combination with cell populations for cell-laden printing include natural, synthetic and hybrid (combination of natural and synthetic) bioinks. The desired material selected according to the functional ultimate use, to try to circumvent inherent material limitations for the printing of living cells.

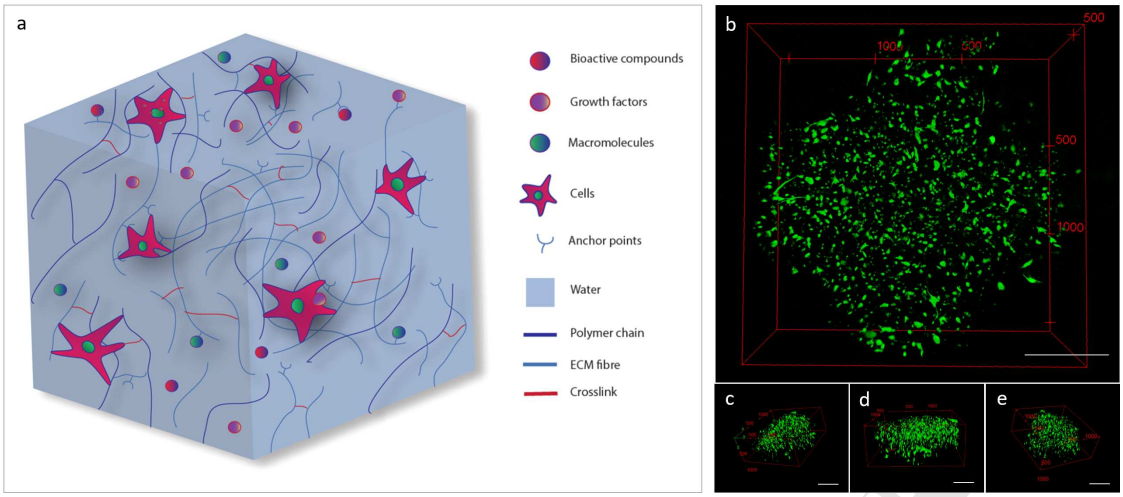

Fig. 2. Hydrogels resembling extracellular matrix. (a) Polymeric cell carrier matrices need to mimic the physiological environment that cells experience and sense within the human body. Cells can use filopodia extensions to attach to several anchor-like proteins within the gel matrix or interact with the polymeric chains. Bioactive compounds, growth factors and macromolecules can be included or preserved from natural tissue to stimulate cell activity or differentiation toward a specific lineage. (b) Skeletal stem cells (SSCs) encapsulated in GelMA hydrogels and printed into a 3D lattice structure. 3D reconstruction of a SSCs-laden cross-section illustrating cells stretching and spreading in three dimensions. Right (c), front (d) and left (e) 3D reconstructions of SSCs encapsulated in printed GelMA demonstrating uniform and consistent cell attachment throughout the cross-section. Scale bars: (b-e) 500 µm.

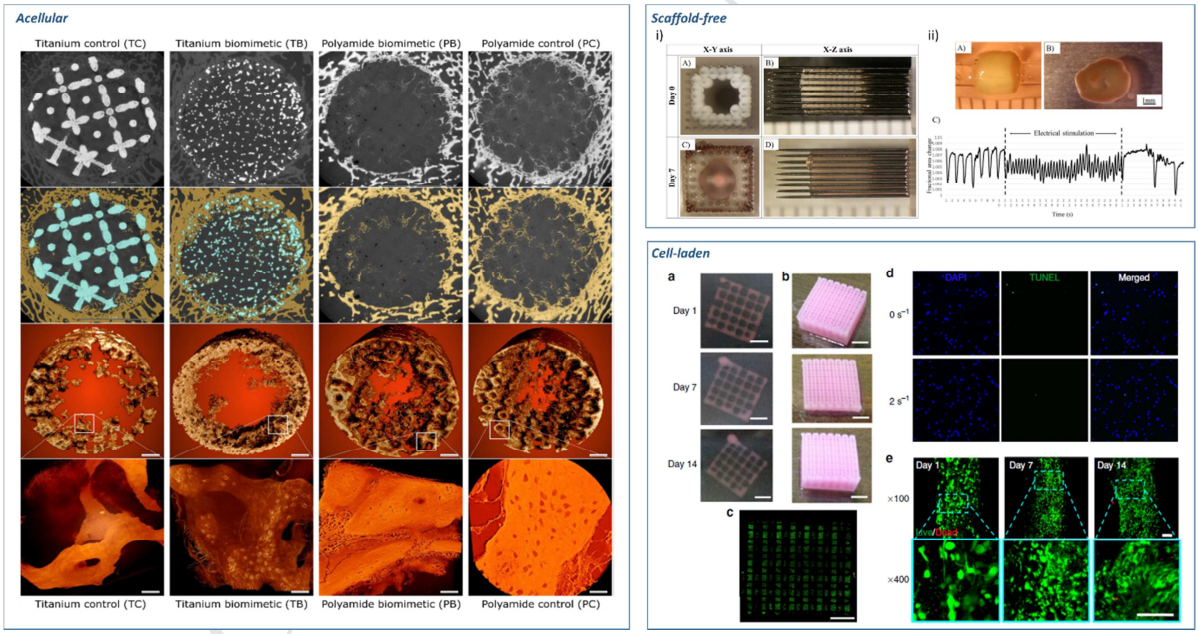

Fig. 3. Current biofabrication approaches. **Acellular**. Reconstruction of bone ingrowth and segmentation of micro CT images of acellular 3D implants in sheep distal femur defect. First and second row: 2D slices of the 3D implant. Bone is labelled in yellow and metal in blue. Third and fourth row: bone ingrowth and close up high resolution detail of nascent bone. Pixel size 0.5 µm, panels' scale bars are 40 µm. Adapted with permission from [39] CC BY license. **Scaffold-free**. i) Scaffold-free tubular cardiac constructs on a needle array. Representative images of tubular constructs just after printing (A,B) and after culture for 7 days (C, D). ii) Needle-free tubular constructs (A) cultured for 7 days (B) and further electrically stimulated and effects analysed (C). Adapted with permission from [46]. **Cell-laden**. Representative images of the whole constructs prepared with hdECM (a) and adECM (b) at progressing days of cell culture. Confocal image of the whole construct prepared with adECM at day 14 of culture (c) showing live cells (green) and dead cells (red) (scale bar, 2 mm). An image of the whole construct reconstructed from B32 images taken at different positions. Representative images of apoptosis through TUNEL (d) and Live/Dead (e) assays. TUNEL assay displays minimal apoptotic cells, indicating the generated stress at 2 s^{-1} shear rate at the nozzle wall did not produce a deleterious effect on the encapsulated cells with comparable apoptosis to the non-printed gel (0 s^{-1}). Cell viability was >95% at day 1 and >90% at both day 7 and 14. Scale bars: (a-c) 2mm, (d,e) 100mm. Adapted from [50] with permission from publisher.

3.2 Hydrogels for Cell Printing - ECM Matrix Biomimetics

Biomaterials selected for cell printing should, ideally, allow the cells to regain their original shape following extrusion through a fine aperture and provide the cells with the appropriate stimuli to induce proliferation and differentiation post printing and preserve the cell spatial location [40,41]. Hydrogels engineered to recapitulate ECM environment, are typically composed of polymeric chains that are often crosslinked with one another [52]. Such ECM resembling hydrogels for cell printing derived from decellularised ECM (dECM) cartilage (cdECM), adipose (adECM) and heart tissues (hdECM) have been investigated by Pati *et al.* [50]. Human adipose-derived stem cells (hASCs) and human inferior turbinate-tissue derived mesenchymal stromal cells (hTMSCs) were used as a model cell line to investigate the inherent phenotype tissue-mimicking gel properties. DECM provided a temperature-sensitive hydrogel gelling at physiological temperatures with >95% cell viability at 24 h. HdECM [53] was used to develop a viable 3D printed patch able to induce a potent angiogenic response and enhance cardiac function *in vivo*. Fedorovich et al. [54] embedded MSCs within a matrigel comprising calcium phosphate (CaP) nanoparticles and investigated their efficacy for bone formation in a subcutaneous mouse model. Calcium phosphate components have been shown to be particularly beneficial for new bone formation both *in vitro* and *in vivo* through the release of calcium and phosphorus ions emphasising the attraction of such an approach. The size requisites to enable extrusion-based systems, typically, force the use of material particles in the nanometres range. *In vitro* investigations demonstrated high MSCs viability and bone formation after 6 weeks, although, only fibrous-like tissue was observed within *in vivo* implants showing lack of the desirable osteoinductive properties.

3.3 Hydrogels - Limitations in Cell Printing Applications

3.3.1 Bioinks Lack Inbuilt Mechanical Support

Cell printing can produce stable implants but these typically, lack any tissue specific mechanical properties. Support materials are often used to provide further mechanical aid to the final 3D printed tissue substitute. To address this issue, a number of groups have employed a hybrid approach, that is. the simultaneous deposition of a cell-laden hydrogel with a supportive material to generate a mechanically competent 3D printed constructs [1,55–59].

Poly(ε-caprolactone) (PCL) is a synthetic polymer capable of withstanding a wide range of external loads in comparison to soft and high water-content gels, although, the requisite high extrusion temperature generally makes PCL unsuitable for cell printing. Even as a mechanically stable material, the hard nature of the PCL surface could result in disruption to soft hydrogels providing a non-homogenous environment for cell expansion (altered cell-surface interaction modulating cell proliferation) [1,50]. While hydrogel viscosity can be tuned and can increase linearly with polymer concentration, care is often required to ensure a cell compatible environment [60] and allow for degradation within a relevant time-frame following

implantation. Recently, Freeman *et al.* [47] defined a printability window by looking at differences in alginate molecular weight (MW) in combination with modulation of ionic crosslinking addition. Varying MW to crosslinking ratio, degradation and encapsulated growth factor release could be tuned according to the specific need of developing a hard or soft region. A further approach to overcome the issue of printing soft hydrogels is to use a gel bath [61–63]. The temporary supportive gel allows aiding printing of low polymeric bioinks, building larger and more complex structures. After printing, the constructs can be crosslinked to enhance further the mechanical properties of the scaffold.

3.3.2 Low Polymeric Content Hydrogels Are Ideal for Cell Printing

Hydrogel stiffness, typically correlated with polymer percentage content, can directly influence cell survival and proliferation rates post-printing. High polymer content hydrogels used for printing can impose higher stress on encapsulated cells than softer hydrogels. Physical stress applied on cells by a stiff hydrogel can prove detrimental for post-print cell viability. Therefore, the optimal biomaterial for cell printing should provide a balance in polymer content ensuring a soft and porous three-dimensional microenvironment where cells can be encapsulated avoiding excessive physical stresses as with high polymer materials [31,64–66]. Hydrogel physical properties such as high polymer content can influence cell survival by hindering nutrient supply and waste removal. Indeed, scaffold porosity is recognised as central to *in vivo* environments to elicit appropriate oxygenation and blood vessel ingrowth. It is well known that scaffold pore sizes can influence rate of diffusion and certain pore sizes) may be optimal for, variously, revascularization (5 µm), skin (20-125 µm) and bone (100-400 µm) regeneration [57]. The specific spatial distance between cells encapsulated within deposited fibres and outer oxygen rich ambient can influence nutrient and waste diffusion however, the very nature of hydrogels, being predominantly water, can generally facilitate this exchange, supporting cells during their proliferation process.

3.3.3 Natural or Synthetic Hydrogels Can Influence Printability and Cell Behaviour

Natural materials, derived from natural polymers, often convey the added advantage of cytocompatibility and the provision of natural cues to provide a favourable microenvironment for cell differentiation [30,33]. Synthetic biomaterials synthesized from polymers or blocks of co-polymers, typically yield more consistent and reproducible structures than natural polymers. Synthetic and natural biomaterials have however been employed as surfactant agents, bio-carriers and support material for several cell lines [31] and can be applied for cell printing application given their viscoelastic mechanical properties and shear thinning behaviour [31,60]. Additionally, hydrogels selected for bioprinting should demonstrate stable gelation conditions to enable even deposition and ensure shape fidelity [67,68]. Hybrid materials can be applied to create optimise inks for encapsulating and printing living cells as they combine the natural and the synthetic components to produce highly printable bioinks [31,69,70].

4. The challenge of cell printing for tissue engineering

The particular target tissue and organ of interest, such as bone and cartilage, will define the selection of cell types required to recapitulate specific biological functions. Cell proliferation rates of the growing tissue substitute need to be tuned to provide the requisite number of cells within the constructs while specific cell migration capability as well as adhesion properties must be considered prior to printing. Cell source, characteristics, functionality all influence cell encapsulation as well as loading density. Furthermore, cell functionality post-printing is strongly influenced by a number of printing parameters.

4.1 Cell Seeding-Encapsulation Protocols for Cell Printing Can Hinder Post-Printing Construct Functionality

Seeding porous scaffolds post-printing is a widely used approach in tissue engineering, but too often leads to impaired cell density distribution resulting, typically, in a higher concentration of cells on the periphery of the construct. Uneven cell seeding produces non-homogenous oxygen gradients from the surface to the core of the scaffold leading to impaired growth [40]. Therefore, technologies such as cell printing with direct patterning and accurate positioning have been evaluated for successful human tissue replication by several groups [1,50,60,67,71]. Incorporation of cells can ensure homogeneous cell distribution compared to routine cell seeding that cannot grant uniform cell distribution within the tissue scaffold. However, the biomaterial of choice can directly influence cell encapsulation. Thermoresponsive and thixotropic hydrogels are preferable given the hydrogel viscosity can be significantly reduced due to thermal or physical stresses, permitting cell suspension inclusion and ensuring low cell damage. Indeed, significant cell death can occur even prior to printing, during the cell-loading step. Crucially, even before printing, the hydrogel moduli affect the cell viability when encapsulated. For example, low moduli hydrogels (<1kPa) can often provide a better environment for cells to attach, expand and proliferate [72,73]. Physically stronger gels can be loaded with cells with the help of mechanical methods (mixing, centrifugation or vortexing) ensuring high printing fidelity, nevertheless cell encapsulation still remains a crucial and unresolved issue.

4.2 Cell Printability and Printing Parameters Influence on 3D Printed Cell-Laden Constructs

Following extrusion, encapsulated cells are subject to constant stresses given their presence in a matrix lattice [9] inducing significant loads on the cells. Moreover, when encapsulated at high-density, cells can experience overcrowding resulting in impaired growth. These observations indicate the need to generate 3D constructs, which are biologically relevant and can be implanted almost immediately into an *in* vivo model. Printability is defined by the rheological properties of the bioink [49]. Prior to printing, a rheological evaluation of the employed hydrogel is essential to understand and tune the

biofabrication parameters to obtain high shape fidelity constructs. However, printability is often the result of a combination of a series of evaluations that remove the beneficial use of a specific hydrogel in combination with a cell type. Mammalian stem cells, in contrast to established cell lines are, typically, particularly sensitive to environmental changes and if, for example, forced through a narrow aperture channel, their membrane integrity, capacity to differentiate and proliferate can be hampered [30,74] necessitating careful consideration of forces, printing parameters and protocols that may induce a low or high degree of cell damage after printing.

4.2.1 Cell Density is Essential for Functionality of Printed Cell-Laden Constructs

Cell density is a crucial parameter in the development of specific tissue substitutes given the direct influence of printable hydrogel physical properties. Indeed, evidence of a reduction in stiffness of cell-laden hydrogels with an increase of cell density content have been recently reported [75,76]. The number of cells encapsulated for printing can affect multiple outcomes post-printing. Printing low-density cell-laden hydrogels can result in poor tissue integration and ingrowth construct. In contrast, deposition of a material containing a high cell density can lead to cell over-accumulation both in the print head and in a small-deposited area resulting in a reduced space for cells to proliferate and remain viable. Therefore, optimal cell concentration upon encapsulation is required before printing, due to the high percentage of cell mortality upon printing that is proportional to nozzle diameter and system pressure employed.

According to the tissue of interest, the cell density employed can vary. Thus, 5-10 × 10^6 cells ml^{-1} has been found to be an optimal concentration for hydrogel encapsulation in bone tissue engineering [9,40,77–79]. Cell content can influence strand deposition as well since high cell concentration in the bioink can lead to polymer relaxation or strengthen the polymer composition dependent on the material used. As shown in Fig. 4a, 3D printed strands that encapsulate various cell densities can lead to different and unexpected results. Low-density cell encapsulation (<1×10^6 cells ml^{-1}) will result in high cell survival due to the protective action of the biopaste in which the cells are encapsulated and increase post-printing proliferation rate. Low cell density can result in reduced cell growth, tissue maturation and integration *in vivo*. Encapsulating at a high cell number (>5×10^6 cells ml^{-1}) will result in swollen and unstable 3D printed strands. Furthermore, high cell content can result in pronounced cell hypoxia, cell saturation and disruptive cell-to-cell interaction. These observations necessitate the need to select the appropriate cell density to address the appropriate biological environment to, for example, facilitate cells anchorage to polymeric matrix filaments, cell-cell interactions in three dimensions and cell proliferation within the 3D matrix.

4.2.2 Shear Stress, Nozzle Shape and Printing Orifice Affect Cell Viability during Printing and Influence Construct Functionality Outcomes

An understanding of the influence of external forces, including shear stress, compression, cavitation, etc. imposed by 3D printing systems on cell viability and

proliferation is pivotal in the printing process [80]. Shear thinning (viscosity decreased by shear) and immediate gelation properties are ideal parameters for biomaterial cell-carrier selection; while extrusion of biomaterials that present shear-thickening (viscosity increased by shear) characteristics along with unfavourable gelling mechanisms affect cell viability resulting in cell death and injury [30]. Shear stress is the specific sum of forces that impose a deformation on a material in a plane parallel to the direction of the stress. These physical forces are of particular interest in cell printing given the shear field that is present at the nozzle is believed to be the main cause for cell damage and loss during printing [49,81,82]. During bioink extrusion from a syringe nozzle, cell mechanical disruption is a direct consequence of shear, where fluid at nozzle walls undergoes shear thinning behaviour while remaining in laminar flow. Blaeser *et al.* [81] investigated the shear forces that induce cell damage in a 3D printing system. By predicting and controlling shear forces applied at the dispensing nozzle, cell survival and proliferation was affected directly by forces in the range between 0.7 and 18 kPa. Shear stress doubled when a more viscous alginate solution (1.5 wt %) was extruded. L929 mouse fibroblast cell viability when subjected to shear forces lower than 5 kPa was observed to be around 96%, and about 91% when exposed at 5-10 kPa stress. Furthermore, cell survival was dramatically reduced (76%) when cells were exposed to forces greater than 10 kPa.

Applied pressure and nozzle inner diameter and shape are the most relevant factors resulting in cell damage when printing cell-laden hydrogels. During the printing process, cells are directly exposed to a velocity gradient profile that changes according to the nozzle employed (typically a maximum intensity at the centre of the nozzle leaving a static field around the nozzle wall) [82]. Therefore, printing parameters need to be adapted according to the desired bioink. For instance, blunt cylindrical nozzles are used to print with high precision, bioinks with and without cells. The cylindrical nozzle design can compromise and affect cells given the high shear stress field that is produced at the luer-lock interface of the nozzle upon printing [64]. Cylindrical nozzles have been substituted with more cell compliant conical-shaped nozzles, as confirmed by recent publications [64,83] where cell viability following extrusion in both type of nozzles was investigated in relation to shear stress and polymer concentration. Cells appear to be less affected by shear imposed by conical rather than cylindrical nozzles. Thus, cell printing using cylindrical nozzles showed an approximate 10 fold decrease in cell viability post-printing in comparison to conical nozzles of identical gauge [64,83].

As illustrated in Fig. 4b, different nozzle apertures can be used to print living cells. Medium size nozzle apertures (i.e. 250-800 µm) can ensure printing fidelity and high cell survival upon extrusion, as the extruded cells are not affected by the particular force fields that developed at the nozzle walls because of hydrogel flow. A large nozzle orifice (i.e. >800 µm) can ensure high post-printing cell survival because of the low shear imposed on the printed cells at the expense of printing resolution. In contrast, a nozzle with a small aperture (i.e. <250 µm) can enable printing of highly precise structures but will impose an elevated stress on printed cells during the printing process. It is thus self-evident that the same numbers of cells in small versus large nozzle environments will be subject to stress imposed by other cells and the repulsive forces from the contact with the near nozzle walls. Recently, Nair *et al.* [80] quantified the short term bioprinting-induced injury experienced by viable cells upon extrusion. Rat adrenal medulla endothelial cells encapsulated within sodium alginate solution were used as a cell-model. Cell fate and morphology were investigated according to the dispensing pressure (5, 10, 20, and 40 psi) and the nozzle diameter (150, 250, and 400µm) parameters used. The study confirmed that viable extruded cell percentage decreased with

increased printing pressure and decreased with a reduction in the nozzle aperture. Alginate-encapsulated cells forced through a 150µm nozzle at 40 psi experienced necrosis rather than apoptosis showing pyknosis and karyolysis morphologies. Aguado *et al*. [84] used primary and established cell lines as models to investigate the biomaterial protection effect that alginate may provide to stem cells upon needle extrusion. The authors found that upon extensional flow, linear fluid velocity could increase rapidly in the nozzle area reaching an almost 300-fold gain during nozzle extrusion causing acute cell death. Indeed, shear rate is estimated to increase during extrusion jumping from roughly 5 s^{-1} to 26 × 10^3 s^{-1}.Interestingy, alginate hydrogel acting as a surfactant agent can limit damage to cells induced by high extrusion pressure compared to cells delivered using buffer controls.

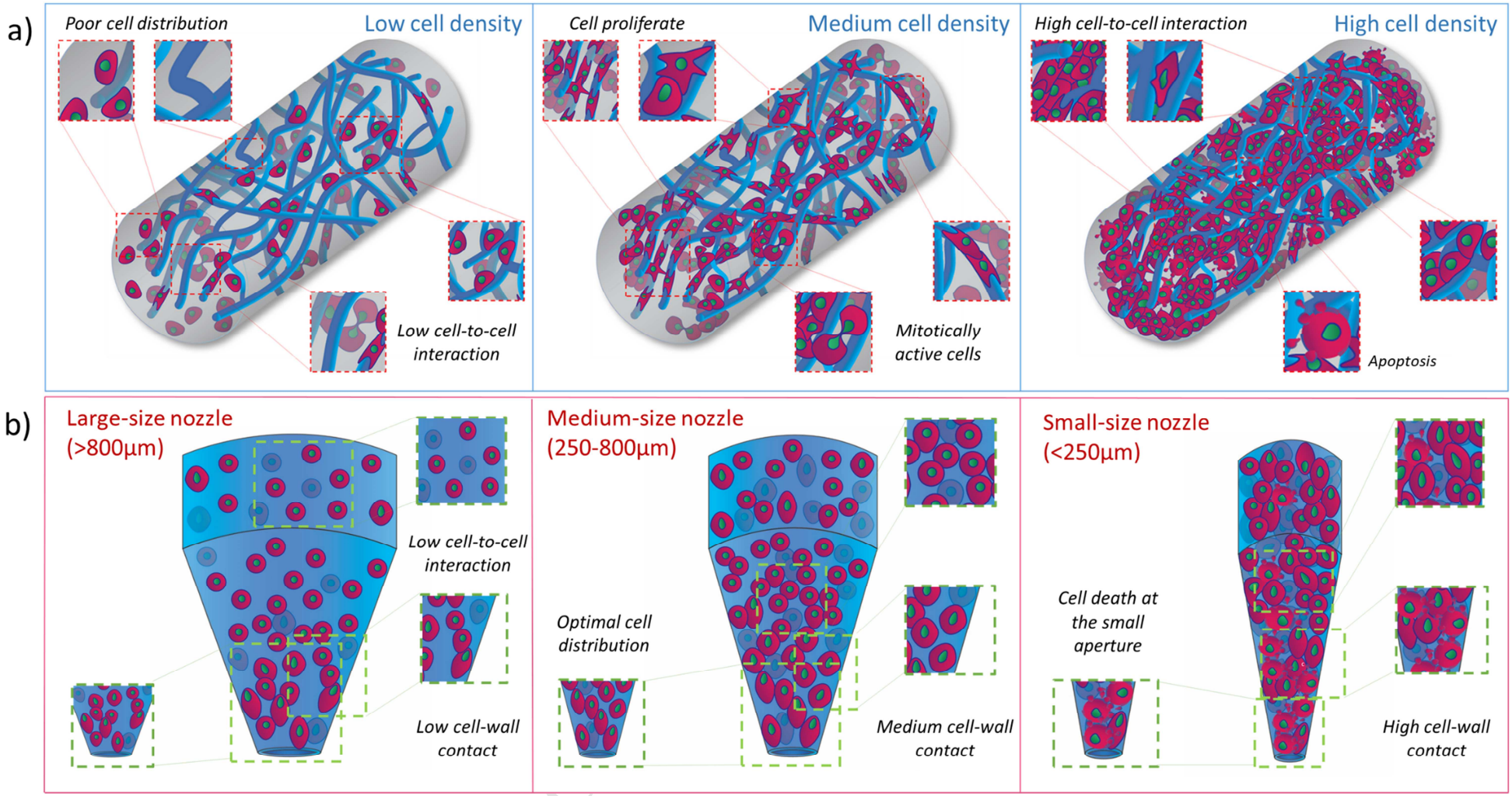

Fig. 4. Cell seeding density influence on 3D cell-laden biomaterial strands and nozzle extrusion. (a) Extruded cell-laden filaments can retain a number of cells proportional to the cell seeding density. Polymeric chains (dark blue) concentration and distribution directly influence cell proliferation capability. A lower cell seeding density results in poor cell distribution within the printed strand showing low cell-to-cell interaction and a limited proliferation rate. Increasing the cell seeding density results in a printed strand filled with cells with a high degree of cell-to-cell interaction and cell death. Proliferation and viability is limited by physical stresses imposed by neighbouring cells. Cell density can be tuned to achieve an even distribution of cell encapsulated within the printed filament in such a way that cells can maintain the required interaction with other cells to remain mitotically active and proliferate. (b) Maintaining constant the number of cells loaded in a printing syringe but changing the nozzle aperture will affect cell printability. Large nozzles (>800µm) allow limited cell-nozzle walls and cell-to-cell interactions resulting in a widespread distribution of cells in suspension within the bioink. These settings can ensure high cell survival upon extrusion but result in low resolution of the overall construct. In contrast, narrower nozzles (<250µm) offering smaller surface area for the same number of cells force biopaste encapsulated cells to interact with one another resulting in high density at the nozzle aperture. A narrow orifice can produce high resolution, as well as high cell death upon printing. Medium size conical nozzles (250µm-800µm) ensure an optimal cells distribution within the nozzle and an increase in print resolution without influencing, extensively, cell survival.

4.2.3 Printing parameters and crosslinking methods influence cell viability

The effects of printing parameters including printing pressure and polymer content on cell viability are illustrated in Fig. 5. Printing pressure can negatively affect cell viability, exacerbated in the presence of cell printing with a high polymer content cell-laden material, extruded at high pressure. In contrast, cells will remain viable if low pressure and low polymer content materials are employed. However, a low content hydrogel will not be sufficiently viscous to enable printing and to retain architectural structure upon extrusion. Thus, innovative engineering techniques, biomaterials and cell-seeding densities, are required to produce viable cell-laden scaffolds. Cross-linking of scaffolds post-printing could provide a reliable methodology for generating enhanced cell viability. Indeed, Lim *et al.* [85] have produced a visible light curing GelMA hydrogel for cell printing. GelMA has gained popularity as biomaterial for cell printing given the potential for radical polymerization-mediated gelation.

GelMA is not only highly biocompatible due to the presence of gelatin within the material but GelMA can also form a strong gel through a post-printing photo-crosslinking processing. UV [86] or visible [85] light activated molecules can functionalize methacryloyl groups with gelatin chains forming strong irreversible covalent bonds. The use of visible light in particular, as a crosslink-mediator involves the photoexitacion of tris(2,2′-bipyridyl)dichlororuthenium(II) hexahydrate (Ru) which is modified from Ru^{2+} to Ru^{3+} through electron donation to sodium persulfate (SPS). This consequently dissociates into sulfate anions causing covalent bonds between methacryloyl groups. Results have demonstrated the incidence of UV-light on cell survival. HAC and MSCs constructs crosslinked at 50 mW/cm^2 light intensity showed poor cell viability when exposed to UV (63% and 67% respectively) after one day. Visible light-crosslinked constructs presented higher cell viability after only one day (83% HAC and 87% MSCs) confirming the toxic effect of UV-curing agents and light.

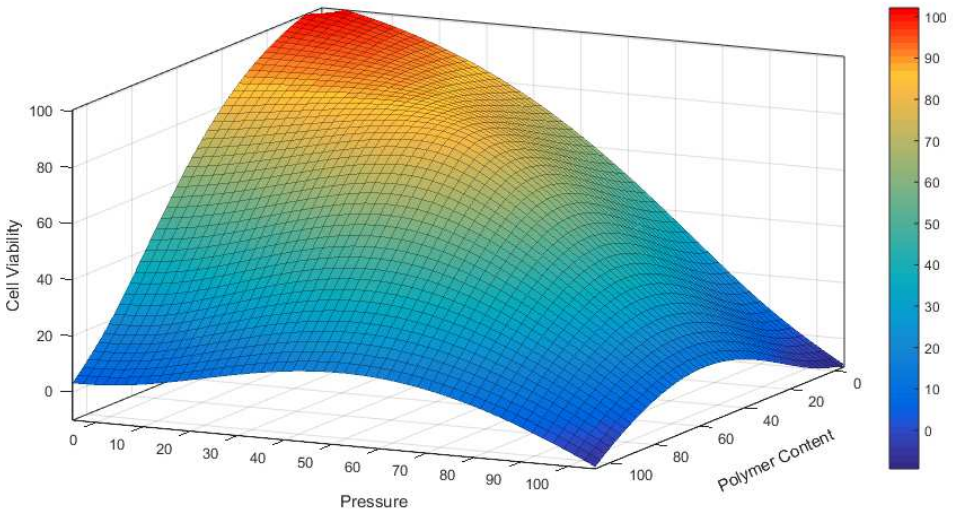

Fig. 5. Three-dimensional diagram showing the correlation between cell viability and pressure provided by the 3D printing system and bioink polymer content. Values listed in percentages. The highest cell viability upon printing is observed when a low polymer content hydrogel is used in combination with low pressure. Increasing polymer content and lowering extrusion

pressure results in the absence of bioink deposition and reduced cell viability upon printing. High pressure and the use of a low polymer content paste for cell encapsulation produces structurally weak scaffolds. Elevated print pressure and polymer content lead to a significant decrease and ultimately, a total loss of viable printed cells. Indicative 3D model plotted with Matlab (MathWorks, R2018a).

4.3 Bioprinting Stem Cells

4.3.1 Printing Stem Cells to Fabricate Functional Tissue

Human-scale tissue 3D printed substitutes have, to date, proved elusive. Indeed, the survival and functionality of the printed cell represents a key challenge in printing large engineered tissue grafts [1]. The use of stem cells has been exemplified as a key factor for human tissue regeneration, with significant potential demonstrated in the reparation of a medium-large portion of outer skin tissue [87]. Indeed, over the last few years, stem cells have been successfully incorporated into 3D printing systems allowing precise cell-patterning and development towards tissue microenvironment recapitulation (summarised in Table 1).

Physical forces involved in the printing process can influence the functionality of stem cell-laden biofabricated constructs [75]. For example, mechanical cues have been shown to direct cell lineage commitment [88]. Shear stress, as a consequence of the printing process, has been shown to impact on cell survival. Recent findings confirm that during physiological remodelling when vascular progenitors are involved, laminar shear stress and cyclic stretch play crucial roles in endothelial and smooth muscle differentiation, respectively [89]. Moreover, it is well-known that skeletal homeostasis is highly influenced by biophysical signals [90,91]. Thus, fluid flow can activate and regulate intracellular signalling cascades in human bone marrow-derived MSCs. Shear-triggered increase in calcium divalent ions mediated by MAP kinase ERK1/2 modulate cell proliferation demonstrating a direct effect of physical stresses on regulation of MSCs proliferation and death [92].

Shear forces involved in the printing process directly correlate with stem cell survival. Low stem cell survival is to be expected when high shear stresses are applied. This is particularly true for embryonic stem cell (ESC) printing [75,93]. Ouyang *et al.* [75] found that printing ESCs at a shear stress lower than 100 Pa, resulted in >90% cell viability. Furthermore, ESCs encapsulated in a gelatin-alginate composite could be printed, avoiding extensive damage, at between 25 - 30℃ and 5 - 8 % gel concen tration indicating the need for selection of hydrogel and printing parameters for the cell type of interest. Indeed, for stem cells to maintain their pluripotency phenotype it is essential to avoid triggers of differentiation upon printing. Faulkner-Jones *et al.* [94] have shown printing of alginate-encapsulated human embryonic stem cells and human induced pluripotent stem cells within defined conditions, derived hepatocyte-like cells (hESC- and hiPSCs - derived HLCs, respectively) could be generated. iPSCs were cultured in differentiation conditions for 6 days, printed and differentiation protocols resumed until day 17. Importantly, hepatic markers expression was maintained post printing, indicating iPSCs could be printed during the differentiation window. The authors reported the use of a long nozzle (24.4 mm) produced 71% cell survival compared to 84% with a short nozzle (8.9 mm). Prolonged pressure conditions were hypothesized to be the cause of such high cell mortality using such a nozzle and for hiPSCs.

The authors indicated optimal printing parameters could be set at around 0.6 bar with application of a short nozzle for cell printing.

4.3.2 Stem Cell Printing: Current Challenges in a Skeletal Tissue Engineering Approach

4.3.2.1 Stem cell density impact 3D printed constructs viability, proliferation and functionality

Evidence indicates that an initial high stem cell density encapsulation in printable hydrogels can lead to enhanced tissue formation [76]. However, the use of elevated stem cell numbers within a bioink can result, for example with human MSCs, in reduced viability and proliferation after printing. In contrast, a low initial cell density can lead to poor functionality [95]. Recently, we have examined the influence of low and high cell density on cell viability and construct functionality after printing (Fig. 6). We used an established bioink system (GelMA) [85], to encapsulate skeletal stem cells at densities not previously examined following literature examination of cell systems that employed high and low [85] cell densities respectively.

Low-density cell printing (≤ 1×10^6 cell ml^{-1}) produced constructs (Fig. 6a) that preserved high cell viability for 21 days in culture [85]. An attraction of such an approach is that modest numbers of skeletal stem cells (SSCs) can be easily generated at low passage numbers (P1) and confluency in flasks, which is important for preserving stemness. SSCs seeded at a low-density (Fig. 6b) displayed cell attachment with limited spreading, due to limited initial number. The results (Fig. 6c) demonstrated an elevated and increasing viability post printing (> 80%) up to 21 days. These low-density constructs could be implanted with the potential to recruit host stem cells to the site of implantation to achieve a functional cell number for optimal conditions for the repair and regeneration of damage tissues. In marked contrast, elevated numbers of encapsulated SSCs (> 5×10^6 cell ml^{-1}) in printed scaffolds (Fig. 6d) resulted viable after printing and their seeding on printed scaffolds confirmed enhanced cell attachment and spreading (Fig. 6e). Elevated cell seeding density has been found to enhance cell-cell communication, which results crucial towards the differentiation into the desired cell type [96]. Printing cells at elevated density has the potential to produce ready-implantable constructs due to an immediate functional response of the printed cell-laden scaffold. Although this is not without its challenges. High SSCs numbers derived from primary isolation, require extensive *in vitro* expansion, which can negatively affect their phenotype. Furthermore, the encapsulation of such elevated cell numbers can affect the nutrient exchange and waste removal from encapsulated cells within the lattice structure, resulting in a significant decrease in cell viability and density after 21 days of culture (Fig. 6f).

Nevertheless, if significant undifferentiated SSCs are encapsulated and preserved in culture with optimal nutrient and gaseous exchange *in situ*, then cell-laden constructs could potentially be used to produce readily available printed implants. Thus, an optimal cell density should be carefully evaluated depending on the bioink of choice to achieve immediate and sustained differentiation and functionality within the implanted cellular printed scaffold.

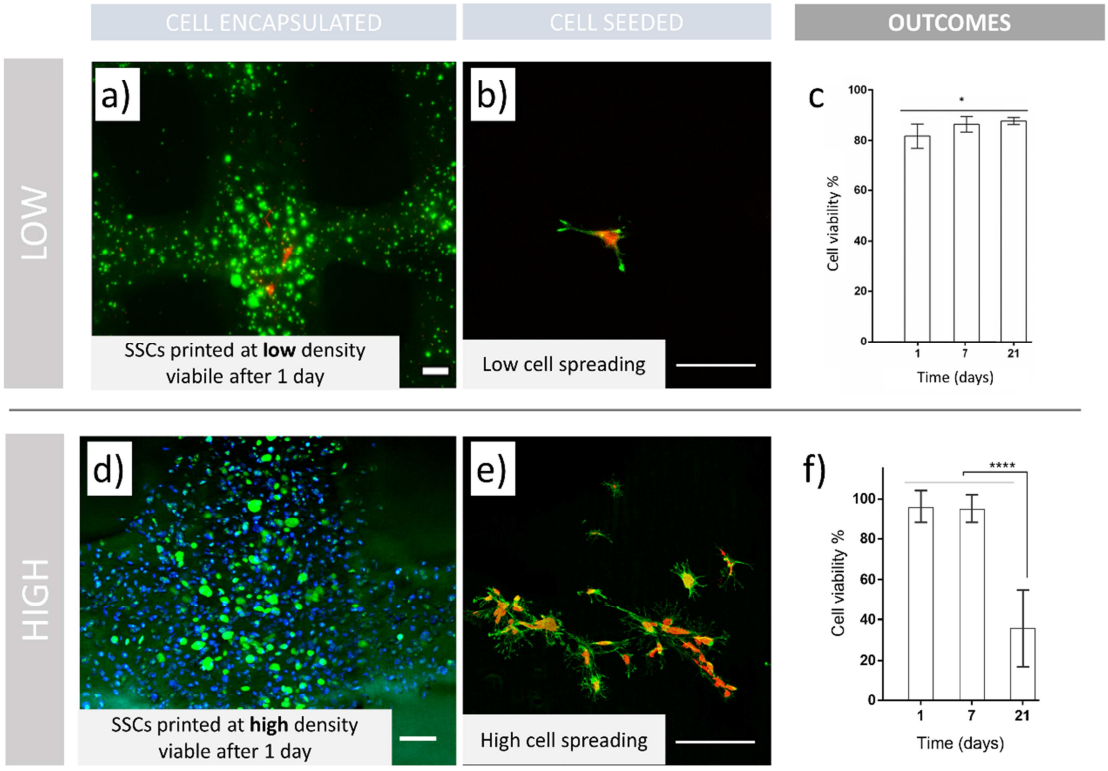

Fig. 6. Viability of 3D constructs fabricated by cell printing depends on initial cell density. SSCs were encapsulated at (a-c) low density (≤ 1×10^6 cell ml^{-1}) and (d-f) high density (> 5×10^6 cell ml^{-1}) GelMA bioinks. (a) Viability of 3D printed GelMA is adapted from [85] (Copyright 2016 American Chemical Society). Living cells are marked green, dead cells in red. (b) Low cell density seeded on 3D printed GelMA scaffolds. (c) Quantification of viability of 3D printed hMSCs in GelMA is adapted from [85] (Copyright 2016 American Chemical Society). (d) High cell density is encapsulated and printed in GelMA bioink. Living cells are in green, pre-labelled cells to visualise distribution in blue – from previously employed protocol [31]. (e) Equal density was seeded on top of the 3D printed scaffolds to show visual comparison between different cell seeding numbers. (f) Viability was determined by confocal microscopy (Leica SPS5) cell counting in a ROI 10×. Pre-encapsulation staining of all cells in blue with lypophilic dye (Vybrant DiD, ThermoFisher) and metabolically active cells in green (Calcein AM, ThermoFisher) was done using previously employed methodology [31]. Statistical analysis was carried out using two-way ANOVA (*p<0.05, **** p<0.0001). Scale bars: (a,d) 200 µm, (b,e) 100 µm.

4.3.2.2 3D printing vasculature: challenges in skeletal biofabrication

Currently, bone defects are, typically, treated with autograft and allograft [97], but an absence of sufficient nutrient supply can lead to necrosis and poor interconnection of the surgical graft. While hypoxic conditions are, in certain contexts, able to enhance proliferation and maintain stemness in stem and progenitor cells [40], oxygen deprivation can also negatively influence tissue development and cell behaviour *in vivo*. Thus, spatial distribution of cells inside a polymeric matrix is important to grant sufficient oxygen delivery to cells. Cell printing strategies can overcome inhomogeneous cell distribution along the implantable constructs overcoming major limitations of static and dynamic cell seeding.

Bone repair capacity is sustained through an appropriate vascular supply, facilitating osteoprogenitor cell recruitment, proliferation and differentiation, gas exchange and bone homeostasis [97]. Kolesky *et al.* [67] showed that centimetre-scale bioprinted 3D cell-laden engineered vascularized tissues could be artificially perfused for more than 6 weeks. Multiple cell types such as HUVECs, HNDFs and MSCs were included within the 3D printed 'bioreactor'. Complex dense vascularized tissues were created in a modular fashion by printing cells in hydrogels with pastes using a silicone ink for support. Synthetic PF127 was used to generate a soluble sacrificial framework, leaving an optimal porosity for HUVECs. Void interconnections between HUVECs vasculature network and MSCs-laden hydrogel were filled with HNDF-laden ink. Results showed that with increasing cell density, MSC viability reduced proportionally with distance from the nearest blood vessel. The authors reported, upon osteogenic conditioning, thick vascularized constructs that differentiated into bone tissue.

The use of MSCs for tissue reparation has typically resulted in the selection of bioinks with low mechanical properties to ensure effective MSC encapsulation and delivery that ensured limited damage. However, hydrogel softness can often induce vertical pores that collapse with consequent loss of pore interconnectivity. This can negatively affect 3D printed cell-laden physical structures and cell viability impacting on oxygen exchange and limiting vascular infiltration [71]. By tuning the hydrogel mechanical properties and scaffold design, Schütz *et al.* [60] produced high definition cell-laden scaffolds to address these issues. Although ideal for cell encapsulation, low-concentration alginate solutions (3 wt %) are not suitable for bioprinting due to the loss of the deposited structure. Thus, MSCs were included within a 1:3 alginate-methylcellulose ratio biopaste before printing. The methylcellulose component acted as a temporary rheology-filler providing a physical aid to cell-biomaterial extrusion, released over time in cell culture conditions. The cell-laden hydrogel constructs retained excellent shape fidelity showing open and interconnect porosity. However, printed constructs displayed poor viability confirming that alginate alone was an inadequate support for cell proliferation.

4.3.2.3 Fabricating functional large constructs for skeletal repair

In developing translational biofabrication applications, large 3D constructs generated at a clinically relevant scale have further advanced the clinical potential of bioprinted implants. While most approaches continue to apply acellular 3D printing strategies, [98,99] there is growing interest in printing skeletal stem cells for the functionalisation of scaffolds aiming for the repair of large bone defects . Recently, critical sized implants comprising of cells were fabricated via an automated assembly process [100]. The authors reported the generation of hybrid structures (Fig. 7 i-iii) by prefabricating 3D scaffolds from thermoplastic materials which served as a scaffold for subsequently injected "micro-tissues" – cellular aggregates pre-cultured under osteogenic and chondrogenic culture conditions. Complex anatomically shaped constructs such as full-scale osteochondral resurfacing scaffolds could be generated and supported long-term micro-tissue fusion, chondrocyte viability and cartilage ECM protein (e.g. glycosaminoglycan (GAG) and aggrecan) deposition *in vitro*. Similarly, Daly *et al.* [101] successfully produced human scale tissue. The use of stiff polymeric printed structures helped to print cellular spheroids within the pores, to guide the growth of newly formed functional cartilage patches for joint resurfacing applications.

An unresolved challenge in the clinical translation of skeletal biofabrication approaches is the generation of a large 3D tissue analogue [67,71,77,102]. Daly et al. [77] proposed a versatile and scalable approach to direct vascular infiltration within implanted scaffolds during bone repair (Fig. 7 iv). A sacrificial hydrogel (Pluronic) was printed to form an intricate yet interconnected structure, before MSC-laden GelMA was cast and UV-cured to generate a complex micro-porous structure. 3D printed structures were implanted in critical sized femoral defects in a rat model, with major vascularisation of the bone defect core region observed at 4 weeks. Such an implant design showed clear clinical potential, facilitating infiltration of vasculature to promote and orchestrate endochondral bone regeneration.

Recent effort has been made to provide a clinically relevant printing tool, capable of delivering *in situ* viable cells directly in the patient. A laser assisted bioprinting (LAB) technology was employed as a printing platform for delivering mouse bone marrow stromal cells in a mouse calvarial defect, demonstrating more than a two-fold beneficial effect (greater bone volume) with printing of stem cells compared to material ink alone [103].

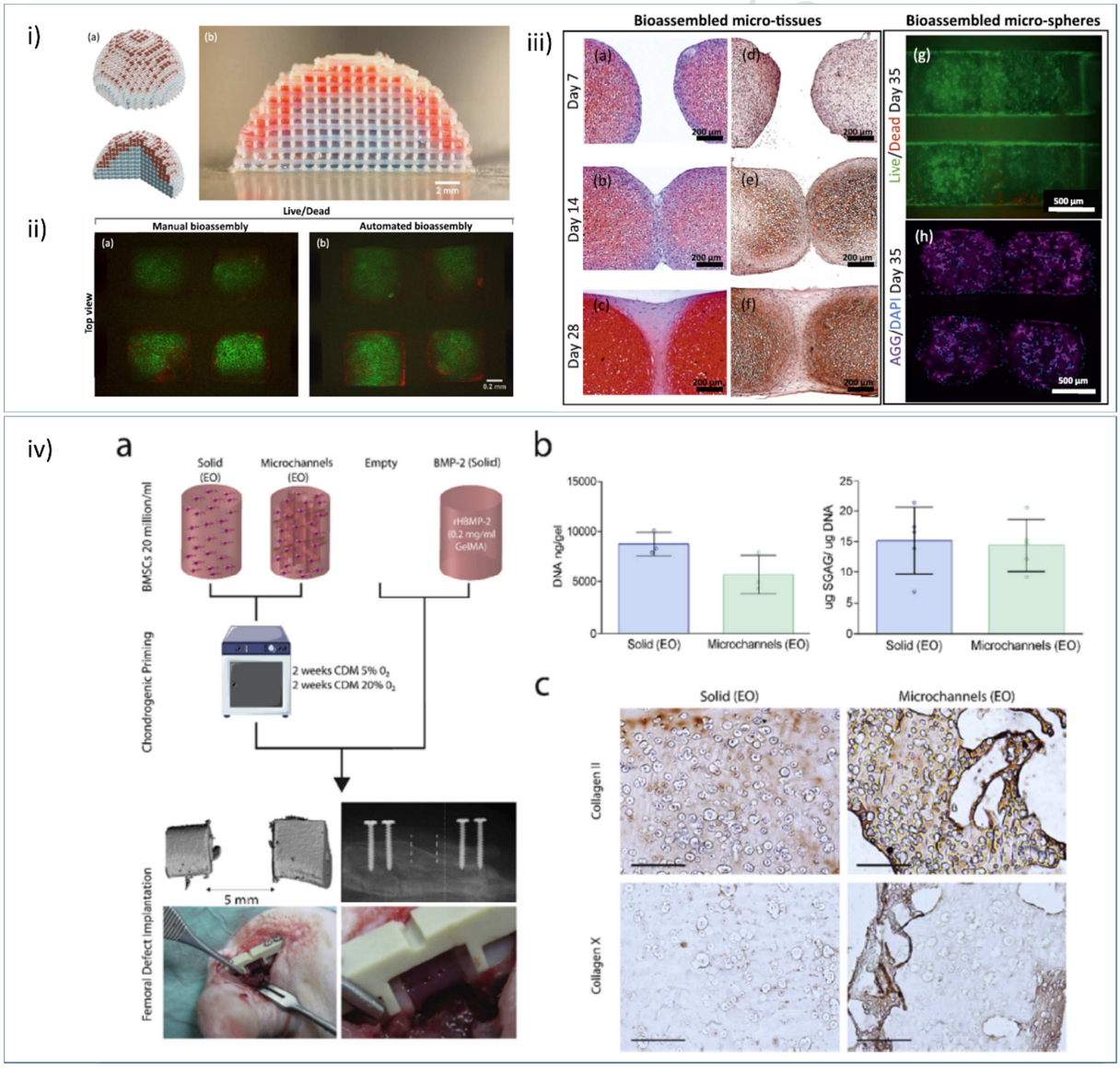

Fig. 7. Scaling up cell printing approaches. (i - a) Illustration of a computer aided design (CAD) example of an assembled hemispherical construct for osteochondral joint resurfacing. (i - b) A biphasic hemispherical construct with stained GelMA

hydrogel micro-spheres representing chondrogenic (red) and osteogenic (blue) phase of an osteochondral construct fabricated by applying the bottom-up automated tissue bioassembly strategy. Scale bars: 2 mm. Fluorescence microscopy images of (ii - a) a manually assembled construct and (ii - b) a construct assembled using the bioassembly system stained with Calcein AM (live cells, green) and Propidium Iodide (dead cells, red). (iii - a-f) Histological analysis of assembled micro-tissues and associated tissue fusion in adjacent culture over 28 days. Histological sections stained with (iii - a-c) Safranin-O/Haematoxylin/fast green or (iii - e, f) Collagen II antibodies. Bioassembled HAC-laden 9.5%GelMA-0.5%HepMA micro-spheres (iii - g, h) stained with Calcein AM (live cells, green) and Propidium Iodide (dead cells, red) (iii - g) or DAPI(blue) and Aggrecan (purple) antibodies (iii - h) after 35 days culture in chondrogenic differentiation media. Adapted with permission [100] CC BY license. (iv - a) Outline of experimental groups (solid and micro channelled) and control groups (empty and BMP-2); pre-implantation chondrogenic culture conditions; and implantation of primed hydrogel (channelled) into a 5mm femoral defect. (iv - b) Biochemical analysis (Total DNA/construct (n=3) and sGAG/DNA (n=5) of both groups after 4 weeks of in vitro culture. (iv - c) Immunohistochemical staining for collagen II pre-implantation, 4× scale-bar 1mm. Adapted with permission [77] CC BY license.

Table 1. Cell printing. *Implants dimensions were not being clearly state in literature. Dimensions evaluation through image analysis have been performed.

Cell line	Density	Biomaterial	Cell survival		Construct Size	In vivo	Printing	Ref.
hMSCs haChs	*in vitro* 5 x 10^6 cells/mL, *in vitro* 3 x 10^6 cells/mL,	Alginate	d0	89%	10 layers, 1X2cm, 10µm layer thickness	mice, subcutaneous (*in vivo* 1X10^7 cells/mL)	BioScaffolder (SYS+ENG)	[71]
HCECs		Gelatin-Alginate + sodium citrate	d0	94.6%	8 layers, 30 X 30 X 3.6mm, 0.8mm layer thickness	X	custom-made	[6]
hChs	10^6 cells/mL	Alginate	d1 d7	90– 94% 93.9%	20 layers, 20 X 20 X 2mm, 250 µm pore size, layer thickness 750µm	X	custom-made: multi-head tissue/organ building system (MtoBS)	[56]
MG63			d1 d7	90–94% 95.6%				
MC3T3-E1	2.3-2.8 × 10^5 /mL	Alginate	d1	84%	27 × 27 X 4.5 mm t) pore size 488µm layer thickness Alginate: 466µm; PCL: 437µm	X	custom-made (melt pot and dispensing system)	[57]
hMSCs and gMSCs cells	5–10 X 10^6 cells/mL	Alginate	porous constructs d3 d7 solid graft d3 d7	 85% 68% 41%	10 X 10 X 1mm pores 0.8 mm (solid) and 2mm (porous) and a fibre height of 100 µm	mice, subcutaneous	BioScaffolder (SYS+ENG)	[40]
hASCs, hTMSCs and L6	1 to 5 x 10^6 cells/mL	decellularized extracellular matrix (dECM)	d1 d7-d14	95% 90%	*hdECM 10 X 10 X 1mm cdECM 6 X 6 X 3mm adECM 10 X 10 X 4mm	X	custom-made: multi-head tissue/organ building system (MtoBS)	[50]
hESC-derived HLCs hiPSC-derived HLCs	1 x 10^7 cells/ml	Alginate	*hESCs 86% hiPSCs 63%		40 layers (13mm)	X	custom-made nanolitre dispensing system	[94]
hMSCs, hNDFs and HUVECs	1 × 10^7 cells/mL	Gelatin–Fibrinogen (hMSCs and hNDFs) Pluronic F127 (HUVECs)	d0	95% (gelatin processing temperature 95°C)	725 × 650 × 125 mm, 100-410µm diameter nozzle	X	custom-made (4 independent printheads)	[67]
HNDFs 10T1 / 2s HUVEC	2 x 10^6 cells/mL	PLURONIC F127, Gelatin Methacrylate (GelMA)	d0 d7 d0 d7	HNDFs 70% 81% 10T/12 61% 82%	*10 X 10 mm, 6 layers height	X	custom-made (4 independent printheads)	[105]
hAFSCs, reChs, C2C12	5 × 10^6 cells/ml 40 × 10^6 cells/ml 3 × 10^6 cells/ml	Gelatin, Hyaluronic Acid, Glycerol, Fibrinogen, Pluronic F127 as sacrificial material	d1 d1 d1	91% 91% 97%	Mandible bone reconstruction 3.6 × 3 × 1.6 cm Ear Cartilage 3.2 × 1.6 × 0.9 cm Skeletal muscle 15 × 5 × 1 mm	Calvarial bone defect 8 mm diameter × 1.2 mm thickness	Integrated Tissue–Organ Printer (ITOP)	[1]
HepG2	1.5 x 10^6 cells/mL	Gelatin Methacrylamide	d0	> 97%	13 X 13 X 1-3 mm thickness, 150-200 µm layer thickness, and fibres spacing of 350 and 550 µm	X	Bioplotter Envisiontec, GmbH	[64]
BMSCs	2.5 x 10^5 cells/mL	Lutrol F127	*Lutrol F 127 d1 d3 d7	 25% 5% 2%	20 X 20mm with spacing between fibres of 300 µm and 150 µm layer thickness	X	Bioplotter Envisiontec, GmbH	[33]
		Matrigel	Matrigel d1 d3 d7	 95%, 90% 98%				
		Alginate	Alginate d1 d3 d7	 90% 90% 97%				
		Methylcellulose	Methylcellulose d1 d3 d7					
		Agarose	Agarose d1 d3 d7	 90% 70% 75%				

5. Summary, Challenges and Future Perspectives

Biofabrication has come to the fore as an innovative engineering strategy for regenerative medicine. In mimicking the three-dimensional microenvironment of human tissue, 3D printed cell implants aim to recapitulate human tissue architecture [71]. Cell printing aims to deliver living cells in a 3D fashion to recapitulate stem cell niches and pathological tissue morphologies for drug screening, or to mimic human tissue complexity working as biologically relevant substitutes. However, improvements from a biocompatibility and mechanics point of view are still required. This will necessitate bioprinting hydrogels to be engineered according to physiological conditions for cell microenvironment to resemble the natural ECM complexity and that provide encapsulation, support and protection [50]. Moreover, cell printing research has yet to fully address pre-printing issues including cell-density seeding and material homogeneity that affect and influence shape fidelity [68], cell viability [81] and functionality [75]. Thus, bioprinted 3D constructs are typically poorly evaluated post-printing for long-term cell survival [49], phenotype maintenance [80] and function [104]. While advances have been made in the development of innovative printing methodologies and new bioinks, pressure [81], shear stress field [49] and nozzle microfluidic dynamics [64] remain key principal engineering paradigms for cell printing applications that have yet to be fully resolved.

There are major hurdles still to be overcome if the potential of stem cell printing is to be realised. These include the challenge of achieving an optimal cell encapsulation density for maximum viability and function, and the requirement for rapid vascularisation of an implanted constructs [67]. Both of these critical challenges will need to be addressed in order to allow production of large cell-laden implants [77,100]. Although numerous approaches have been implemented to produce viable 3D constructs [77,100,105] in vitro, demonstration of *in vivo* functionality in many cases remains to be achieved. Nevertheless, while the full biological potential for 3D printed implantable tissue substitutes remains unclear, the future is bright for the development of human implantable printed constructs and, new developments in bioprinting and bioinks, auger well for the field of regenerative medicine.

Acknowledgements

The work carried out in the author's laboratory was supported by grants from the Biotechnology and Biological Sciences Research Council UK (BB/ L00609X, BB/LO21072/1, BB/P017711/1), UK Regenerative Medicine Platform Hub Acellular / Smart Materials - 3D Architecture: MR/R015651/1 and University of Southampton IfLS, FortisNet and Postgraduate awards to ROCO. The authors would like to thank Professor Michael Gelinsky (TU Dresden) and Professor Tim Woodfield (University of Otago) for useful discussions and fruitful collaborations as well as Prof Shoufeng Yang (KU Leuven) for discussions and access to the extrusion bioprinter. The authors also acknowledge useful discussions related to this paper with Dr Robin Rumney (University of Portsmouth), Dr Stuart Lanham, Dr Janos Kanczler and Dr Yang-Hee Kim (University of Southampton).

References

[1] H.-W. Kang, S.J. Lee, I.K. Ko, C. Kengla, J.J. Yoo, A. Atala, A 3D bioprinting system to produce human-scale tissue constructs with structural integrity, Nat. Biotechnol. 34 (2016) 312–319. doi:10.1038/nbt.3413.

[2] R.J. Klebe, Cytoscribing: A method for micropositioning cells and the construction of two- and three-dimensional synthetic tissues, Exp. Cell Res. 179 (1988) 362–373. doi:10.1016/0014-4827(88)90275-3.

[3] S. V Murphy, A. Atala, 3D bioprinting of tissues and organs, Nat. Biotechnol. 32 (2014) 773–785. doi:10.1038/nbt.2958.

[4] M.J.P. Biggs, R.G. Richards, N. Gadegaard, C.D.W. Wilkinson, R.O.C. Oreffo, M.J. Dalby, The use of nanoscale topography to modulate the dynamics of adhesion formation in primary osteoblasts and ERK/MAPK signalling in STRO-1+ enriched skeletal stem cells, Biomaterials. 30 (2009) 5094–5103. doi:10.1016/j.biomaterials.2009.05.049.

[5] S. Hong, D. Sycks, H.F. Chan, S. Lin, G.P. Lopez, F. Guilak, K.W. Leong, X. Zhao, 3D Printing: 3D Printing of Highly Stretchable and Tough Hydrogels into Complex, Cellularized Structures (Adv. Mater. 27/2015), Adv. Mater. 27 (2015) 4034–4034. doi:10.1002/adma.201570182.

[6] Z. Wu, X. Su, Y. Xu, B. Kong, W. Sun, S. Mi, Bioprinting three-dimensional cell-laden tissue constructs with controllable degradation, Sci. Rep. 6 (2016) 24474. doi:10.1038/srep24474.

[7] M. Schaffner, P.A. Rühs, F. Coulter, S. Kilcher, A.R. Studart, 3D printing of bacteria into functional complex materials, Sci. Adv. 3 (2017) eaao6804. doi:10.1126/sciadv.aao6804.

[8] L. Koch, M. Gruene, C. Unger, B. Chichkov, Laser Assisted Cell Printing, Curr. Pharm. Biotechnol. 14 (2013) 91–97. doi:10.2174/138920113804805368.

[9] G.D. Nicodemus, S.J. Bryant, Cell Encapsulation in Biodegradable Hydrogels for Tissue Engineering Applications, Tissue Eng. Part B Rev. 14 (2008) 149–165. doi:10.1089/ten.teb.2007.0332.

[10] J.I. Dawson, J.M. Kanczler, X.B. Yang, G.S. Attard, R.O.C. Oreffo, Clay Gels For the Delivery of Regenerative Microenvironments, Adv. Mater. 23 (2011) 3304–3308. doi:10.1002/adma.201100968.

[11] D.J. Odde, M.J. Renn, Laser-guided direct writing of living cells, Biotechnol. Bioeng. 67 (2000) 312–318. doi:10.1002/(SICI)1097-0290(20000205)67:3<312::AID-BIT7>3.0.CO;2-F.

[12] R.H. Crawford, J.J. Beaman, C. Cavello, J. Jackson, L.E. Weiss, C.. Séquin, Solid freeform fabrication: A new manufacturing paradigm, IEEE Spectr. 36 (1999) 35–43.

[13] G. Vozzi, A. Previti, D. De Rossi, A. Ahluwalia, Microsyringe-Based Deposition of Two-Dimensional and Three-Dimensional Polymer Scaffolds with a Well-Defined Geometry for Application to Tissue Engineering, Tissue Eng. 8 (2002) 1089–1098. doi:10.1089/107632702320934182.

[14] W.C. Wilson, T. Boland, Cell and organ printing 1: Protein and cell printers, Anat. Rec. 272A (2003) 491–496. doi:10.1002/ar.a.10057.

[15] T. Boland, V. Mironov, A. Gutowska, E.A. Roth, R.R. Markwald, Cell and organ

printing 2: Fusion of cell aggregates in three-dimensional gels, Anat. Rec. 272A (2003) 497–502. doi:10.1002/ar.a.10059.

[16] T. Xu, H. Kincaid, A. Atala, J.J. Yoo, High-Throughput Production of Single-Cell Microparticles Using an Inkjet Printing Technology, J. Manuf. Sci. Eng. 130 (2008) 021017. doi:10.1115/1.2903064.

[17] T. Xu, J. Olson, W. Zhao, A. Atala, J.-M. Zhu, J.J. Yoo, Characterization of Cell Constructs Generated With Inkjet Printing Technology Using In Vivo Magnetic Resonance Imaging, J. Manuf. Sci. Eng. 130 (2008) 021013. doi:10.1115/1.2902857.

[18] R.E. Saunders, B. Derby, Inkjet printing biomaterials for tissue engineering: bioprinting, Int. Mater. Rev. 59 (2014) 430–448. doi:10.1179/1743280414Y.0000000040.

[19] G. Gao, A.F. Schilling, K. Hubbell, T. Yonezawa, D. Truong, Y. Hong, G. Dai, X. Cui, Improved properties of bone and cartilage tissue from 3D inkjet-bioprinted human mesenchymal stem cells by simultaneous deposition and photocrosslinking in PEG-GelMA, Biotechnol. Lett. 37 (2015) 2349–2355. doi:10.1007/s10529-015-1921-2.

[20] G. Gao, T. Yonezawa, K. Hubbell, G. Dai, X. Cui, Inkjet-bioprinted acrylated peptides and PEG hydrogel with human mesenchymal stem cells promote robust bone and cartilage formation with minimal printhead clogging, Biotechnol. J. 10 (2015) 1568–1577. doi:10.1002/biot.201400635.

[21] A. Negro, T. Cherbuin, M.P. Lutolf, 3D Inkjet Printing of Complex, Cell-Laden Hydrogel Structures, Sci. Rep. 8 (2018) 17099. doi:10.1038/s41598-018-35504-2.

[22] C.L. Hedegaard, E.C. Collin, C. Redondo-Gómez, L.T.H. Nguyen, K.W. Ng, A.A. Castrejón-Pita, J.R. Castrejón-Pita, A. Mata, Hydrodynamically Guided Hierarchical Self-Assembly of Peptide-Protein Bioinks, Adv. Funct. Mater. 28 (2018) 1703716. doi:10.1002/adfm.201703716.

[23] M. Gruene, A. Deiwick, L. Koch, S. Schlie, C. Unger, N. Hofmann, I. Bernemann, B. Glasmacher, B. Chichkov, Laser Printing of Stem Cells for Biofabrication of Scaffold-Free Autologous Grafts, Tissue Eng. Part C Methods. 17 (2011) 79–87. doi:10.1089/ten.tec.2010.0359.

[24] R. Xiong, Z. Zhang, W. Chai, Y. Huang, D.B. Chrisey, Freeform drop-on-demand laser printing of 3D alginate and cellular constructs, Biofabrication. 7 (2015) 045011. doi:10.1088/1758-5090/7/4/045011.

[25] S. Catros, B. Guillotin, M. Bačáková, J.-C. Fricain, F. Guillemot, Effect of laser energy, substrate film thickness and bioink viscosity on viability of endothelial cells printed by Laser-Assisted Bioprinting, Appl. Surf. Sci. 257 (2011) 5142–5147. doi:10.1016/j.apsusc.2010.11.049.

[26] M. Gruene, M. Pflaum, C. Hess, S. Diamantouros, S. Schlie, A. Deiwick, L. Koch, M. Wilhelmi, S. Jockenhoevel, A. Haverich, B. Chichkov, Laser Printing of Three-Dimensional Multicellular Arrays for Studies of Cell–Cell and Cell–Environment Interactions, Tissue Eng. Part C Methods. 17 (2011) 973–982. doi:10.1089/ten.tec.2011.0185.

[27] X. Ma, X. Qu, W. Zhu, Y.-S. Li, S. Yuan, H. Zhang, J. Liu, P. Wang, C.S.E. Lai, F. Zanella, G.-S. Feng, F. Sheikh, S. Chien, S. Chen, Deterministically patterned biomimetic human iPSC-derived hepatic model via rapid 3D bioprinting, Proc. Natl. Acad. Sci. 113 (2016) 2206–2211. doi:10.1073/pnas.1524510113.

[28] S.H. Kim, Y.K. Yeon, J.M. Lee, J.R. Chao, Y.J. Lee, Y.B. Seo, M.T. Sultan, O.J. Lee,

J.S. Lee, S. Yoon, I.-S. Hong, G. Khang, S.J. Lee, J.J. Yoo, C.H. Park, Precisely printable and biocompatible silk fibroin bioink for digital light processing 3D printing, Nat. Commun. 9 (2018) 1620. doi:10.1038/s41467-018-03759-y.

[29] K.S. Lim, R. Levato, P.F. Costa, M.D. Castilho, C.R. Alcala-Orozco, K.M.A. van Dorenmalen, F.P.W. Melchels, D. Gawlitta, G.J. Hooper, J. Malda, T.B.F. Woodfield, Bio-resin for high resolution lithography-based biofabrication of complex cell-laden constructs, Biofabrication. 10 (2018) 034101. doi:10.1088/1758-5090/aac00c.

[30] Y. Zhao, Y. Li, S. Mao, W. Sun, R. Yao, The influence of printing parameters on cell survival rate and printability in microextrusion-based 3D cell printing technology, Biofabrication. 7 (2015) 045002. doi:10.1088/1758-5090/7/4/045002.

[31] T. Ahlfeld, G. Cidonio, D. Kilian, S. Duin, A.R. Akkineni, J.I. Dawson, S. Yang, A. Lode, R.O.C. Oreffo, M. Gelinsky, Development of a clay based bioink for 3D cell printing for skeletal application, Biofabrication. 9 (2017) 034103. doi:10.1088/1758-5090/aa7e96.

[32] I.T. Ozbolat, M. Hospodiuk, Current advances and future perspectives in extrusion-based bioprinting, Biomaterials. 76 (2016) 321–343. doi:10.1016/j.biomaterials.2015.10.076.

[33] N.E. Fedorovich, J.R. De Wijn, A.J. Verbout, J. Alblas, W.J.A. Dhert, Three-Dimensional Fiber Deposition of Cell-Laden, Viable, Patterned Constructs for Bone Tissue Printing, Tissue Eng. Part A. 14 (2008) 127–133. doi:10.1089/ten.a.2007.0158.

[34] X. Lu, Y. Lee, S. Yang, Y. Hao, J.R.G. Evans, C.G. Parini, Fine lattice structures fabricated by extrusion freeforming: Process variables, J. Mater. Process. Technol. 209 (2009) 4654–4661. doi:10.1016/j.jmatprotec.2008.11.039.

[35] S. Yang, H. Yang, X. Chi, J.R.G. Evans, I. Thompson, R.J. Cook, P. Robinson, Rapid prototyping of ceramic lattices for hard tissue scaffolds, Mater. Des. 29 (2008) 1802–1809. doi:10.1016/j.matdes.2008.03.024.

[36] D.M. Gibbs, M. Vaezi, S. Yang, R.O. Oreffo, Hope versus hype: what can additive manufacturing realistically offer trauma and orthopedic surgery?, Regen. Med. 9 (2014) 535–549. doi:10.2217/rme.14.20.

[37] M.J. Sawkins, W. Bowen, P. Dhadda, H. Markides, L.E. Sidney, A.J. Taylor, F.R.A.J. Rose, S.F. Badylak, K.M. Shakesheff, L.J. White, Hydrogels derived from demineralized and decellularized bone extracellular matrix, Acta Biomater. 9 (2013) 7865–7873. doi:10.1016/j.actbio.2013.04.029.

[38] F. Pati, J.-H. Shim, J.-S. Lee, D.-W. Cho, 3D printing of cell-laden constructs for heterogeneous tissue regeneration, Manuf. Lett. 1 (2013) 49–53. doi:10.1016/j.mfglet.2013.09.004.

[39] N. Reznikov, O.R. Boughton, S. Ghouse, A.E. Weston, L. Collinson, G.W. Blunn, J.R.T. Jeffers, J.P. Cobb, M.M. Stevens, Individual response variations in scaffold-guided bone regeneration are determined by independent strain- and injury-induced mechanisms, Biomaterials. 194 (2019) 183–194. doi:10.1016/j.biomaterials.2018.11.026.

[40] N.E. Fedorovich, E. Kuipers, D. Gawlitta, W.J. a. Dhert, J. Alblas, Scaffold Porosity and Oxygenation of Printed Hydrogel Constructs Affect Functionality of Embedded Osteogenic Progenitors, Tissue Eng. Part A. 17 (2011) 2473–2486. doi:10.1089/ten.tea.2011.0001.

[41] L. Li, J. Li, J. Guo, H. Zhang, X. Zhang, C. Yin, L. Wang, Y. Zhu, Q. Yao, 3D

Molecularly Functionalized Cell□Free Biomimetic Scaffolds for Osteochondral Regeneration, Adv. Funct. Mater. 29 (2019) 1807356. doi:10.1002/adfm.201807356.

[42] W.-G. La, J. Jang, B.S. Kim, M.S. Lee, D.-W. Cho, H.S. Yang, Systemically replicated organic and inorganic bony microenvironment for new bone formation generated by a 3D printing technology, RSC Adv. 6 (2016) 11546–11553. doi:10.1039/C5RA20218C.

[43] C. Weinand, R. Gupta, A.Y. Huang, E. Weinberg, I. Madisch, R.A. Qudsi, C.M. Neville, I. Pomerantseva, J.P. Vacanti, Comparison of Hydrogels in the In Vivo Formation of Tissue-Engineered Bone Using Mesenchymal Stem Cells and Beta-Tricalcium Phosphate, Tissue Eng. 13 (2007) 757–765. doi:10.1089/ten.2006.0083.

[44] C. Norotte, F.S. Marga, L.E. Niklason, G. Forgacs, Scaffold-free vascular tissue engineering using bioprinting, Biomaterials. 30 (2009) 5910–5917. doi:10.1016/j.biomaterials.2009.06.034.

[45] D. Taniguchi, K. Matsumoto, T. Tsuchiya, R. Machino, Y. Takeoka, A. Elgalad, K. Gunge, K. Takagi, Y. Taura, G. Hatachi, N. Matsuo, N. Yamasaki, K. Nakayama, T. Nagayasu, Scaffold-free trachea regeneration by tissue engineering with bio-3D printing, Interact. Cardiovasc. Thorac. Surg. 26 (2018) 745–752. doi:10.1093/icvts/ivx444.

[46] K. Arai, D. Murata, A.R. Verissimo, Y. Mukae, M. Itoh, A. Nakamura, S. Morita, K. Nakayama, Fabrication of scaffold-free tubular cardiac constructs using a Bio-3D printer, PLoS One. 13 (2018) e0209162. doi:10.1371/journal.pone.0209162.

[47] F.E. Freeman, D.J. Kelly, Tuning Alginate Bioink Stiffness and Composition for Controlled Growth Factor Delivery and to Spatially Direct MSC Fate within Bioprinted Tissues, Sci. Rep. 7 (2017) 17042. doi:10.1038/s41598-017-17286-1.

[48] R. Chang, J. Nam, W. Sun, Effects of Dispensing Pressure and Nozzle Diameter on Cell Survival from Solid Freeform Fabrication–Based Direct Cell Writing, Tissue Eng. Part A. 14 (2008) 41–48. doi:10.1089/ten.a.2007.0004.

[49] N. Paxton, W. Smolan, T. Böck, F. Melchels, J. Groll, T. Jungst, Proposal to assess printability of bioinks for extrusion-based bioprinting and evaluation of rheological properties governing bioprintability, Biofabrication. 9 (2017) 044107. doi:10.1088/1758-5090/aa8dd8.

[50] F. Pati, J. Jang, D.-H. Ha, S. Won Kim, J.-W. Rhie, J.-H. Shim, D.-H. Kim, D.-W. Cho, Printing three-dimensional tissue analogues with decellularized extracellular matrix bioink, Nat. Commun. 5 (2014) 3935. doi:10.1038/ncomms4935.

[51] M.S. Shoichet, R.H. Li, M.L. White, S.R. Winn, Stability of hydrogels used in cell encapsulation: An in vitro comparison of alginate and agarose, Biotechnol. Bioeng. 50 (1996) 374–381. doi:10.1002/(SICI)1097-0290(19960520)50:4<374::AID-BIT4>3.0.CO;2-I.

[52] S. V. Murphy, A. Skardal, A. Atala, Evaluation of hydrogels for bio-printing applications, J. Biomed. Mater. Res. Part A. 101A (2013) 272–284. doi:10.1002/jbm.a.34326.

[53] J. Jang, H.-J. Park, S.-W. Kim, H. Kim, J.Y. Park, S.J. Na, H.J. Kim, M.N. Park, S.H. Choi, S.H. Park, S.W. Kim, S.-M. Kwon, P.-J. Kim, D.-W. Cho, 3D printed complex tissue construct using stem cell-laden decellularized extracellular matrix bioinks for cardiac repair, Biomaterials. 112 (2017) 264–274. doi:10.1016/j.biomaterials.2016.10.026.

[54] N.E. Fedorovich, S.C. Leeuwenburgh, Y.J.M. van der Helm, J. Alblas, W.J.A. Dhert,

The osteoinductive potential of printable, cell-laden hydrogel-ceramic composites, J. Biomed. Mater. Res. Part A. 100 A (2012) n/a-n/a. doi:10.1002/jbm.a.34171.

[55] W. Schuurman, V. Khristov, M.W. Pot, P.R. van Weeren, W.J. a Dhert, J. Malda, Bioprinting of hybrid tissue constructs with tailorable mechanical properties, Biofabrication. 3 (2011) 021001. doi:10.1088/1758-5082/3/2/021001.

[56] J.-H. Shim, J.-S. Lee, J.Y. Kim, D.-W. Cho, Bioprinting of a mechanically enhanced three-dimensional dual cell-laden construct for osteochondral tissue engineering using a multi-head tissue/organ building system, J. Micromechanics Microengineering. 22 (2012) 085014. doi:10.1088/0960-1317/22/8/085014.

[57] H. Lee, S. Ahn, L.J. Bonassar, G. Kim, Cell(MC3T3-E1)-Printed Poly(ϵ -caprolactone)/Alginate Hybrid Scaffolds for Tissue Regeneration, Macromol. Rapid Commun. 34 (2013) 142–149. doi:10.1002/marc.201200524.

[58] J.-H. Shim, K.-M. Jang, S.K. Hahn, J.Y. Park, H. Jung, K. Oh, K.M. Park, J. Yeom, S.H. Park, S.W. Kim, J.H. Wang, K. Kim, D.-W. Cho, Three-dimensional bioprinting of multilayered constructs containing human mesenchymal stromal cells for osteochondral tissue regeneration in the rabbit knee joint, Biofabrication. 8 (2016) 014102. doi:10.1088/1758-5090/8/1/014102.

[59] W. Schuurman, P.A. Levett, M.W. Pot, P.R. van Weeren, W.J.A. Dhert, D.W. Hutmacher, F.P.W. Melchels, T.J. Klein, J. Malda, Gelatin-Methacrylamide Hydrogels as Potential Biomaterials for Fabrication of Tissue-Engineered Cartilage Constructs, Macromol. Biosci. 13 (2013) 551–561. doi:10.1002/mabi.201200471.

[60] K. Schütz, A.-M. Placht, B. Paul, B. Brüggemeier, M. Gelinsky, A. Lode, Three-dimensional plotting of a cell-laden alginate/ methylcellulose blend: towards biofabrication of tissue engineering constructs with clinically relevant dimensions, J. Tissue Eng. Regen. Med. 2 (2015) 408–417. doi:10.1002/term.

[61] S.R. Moxon, M.E. Cooke, S.C. Cox, M. Snow, L. Jeys, S.W. Jones, A.M. Smith, L.M. Grover, Suspended Manufacture of Biological Structures, Adv. Mater. 29 (2017) 1605594. doi:10.1002/adma.201605594.

[62] Y. Jin, A. Compaan, W. Chai, Y. Huang, Functional Nanoclay Suspension for Printing-Then-Solidification of Liquid Materials, ACS Appl. Mater. Interfaces. 9 (2017) 20057–20066. doi:10.1021/acsami.7b02398.

[63] T. Bhattacharjee, S.M. Zehnder, K.G. Rowe, S. Jain, R.M. Nixon, W.G. Sawyer, T.E. Angelini, Writing in the granular gel medium, Sci. Adv. 1 (2015) e1500655. doi:10.1126/sciadv.1500655.

[64] T. Billiet, E. Gevaert, T. De Schryver, M. Cornelissen, P. Dubruel, The 3D printing of gelatin methacrylamide cell-laden tissue-engineered constructs with high cell viability, Biomaterials. 35 (2014) 49–62. doi:10.1016/j.biomaterials.2013.09.078.

[65] H.J. Kong, M.K. Smith, D.J. Mooney, Designing alginate hydrogels to maintain viability of immobilized cells, Biomaterials. 24 (2003) 4023–4029. doi:10.1016/S0142-9612(03)00295-3.

[66] D. Nguyen, D.A. Hägg, A. Forsman, J. Ekholm, P. Nimkingratana, C. Brantsing, T. Kalogeropoulos, S. Zaunz, S. Concaro, M. Brittberg, A. Lindahl, P. Gatenholm, A. Enejder, S. Simonsson, Cartilage Tissue Engineering by the 3D Bioprinting of iPS Cells in a Nanocellulose/Alginate Bioink, Sci. Rep. 7 (2017) 658. doi:10.1038/s41598-017-00690-y.

[67] D.B. Kolesky, K.A. Homan, M.A. Skylar-Scott, J.A. Lewis, Three-dimensional

bioprinting of thick vascularized tissues, Proc. Natl. Acad. Sci. 113 (2016) 3179–3184. doi:10.1073/pnas.1521342113.

[68] A. Ribeiro, M.M. Blokzijl, R. Levato, C.W. Visser, M. Castilho, W.E. Hennink, T. Vermonden, J. Malda, Assessing bioink shape fidelity to aid material development in 3D bioprinting, Biofabrication. 10 (2017) 014102. doi:10.1088/1758-5090/aa90e2.

[69] J. Yin, M. Yan, Y. Wang, J. Fu, H. Suo, 3D Bioprinting of Low-Concentration Cell-Laden Gelatin Methacrylate (GelMA) Bioinks with a Two-Step Cross-linking Strategy, ACS Appl. Mater. Interfaces. 10 (2018) 6849–6857. doi:10.1021/acsami.7b16059.

[70] D. Chimene, C.W. Peak, J.L. Gentry, J.K. Carrow, L.M. Cross, E. Mondragon, G.B. Cardoso, R. Kaunas, A.K. Gaharwar, Nanoengineered Ionic–Covalent Entanglement (NICE) Bioinks for 3D Bioprinting, ACS Appl. Mater. Interfaces. 10 (2018) 9957–9968. doi:10.1021/acsami.7b19808.

[71] N.E. Fedorovich, W. Schuurman, H.M. Wijnberg, H.-J. Prins, P.R. van Weeren, J. Malda, J. Alblas, W.J.A. Dhert, Biofabrication of Osteochondral Tissue Equivalents by Printing Topologically Defined, Cell-Laden Hydrogel Scaffolds, Tissue Eng. Part C Methods. 18 (2012) 33–44. doi:10.1089/ten.tec.2011.0060.

[72] R. Goldshmid, D. Seliktar, Hydrogel Modulus Affects Proliferation Rate and Pluripotency of Human Mesenchymal Stem Cells Grown in Three-Dimensional Culture, ACS Biomater. Sci. Eng. 3 (2017) 3433–3446. doi:10.1021/acsbiomaterials.7b00266.

[73] A. Banerjee, M. Arha, S. Choudhary, R.S. Ashton, S.R. Bhatia, D. V. Schaffer, R.S. Kane, The influence of hydrogel modulus on the proliferation and differentiation of encapsulated neural stem cells, Biomaterials. 30 (2009) 4695–4699. doi:10.1016/j.biomaterials.2009.05.050.

[74] K.H. Kang, L. a Hockaday, J.T. Butcher, Quantitative optimization of solid freeform deposition of aqueous hydrogels., Biofabrication. 5 (2013) 035001. doi:10.1088/1758-5082/5/3/035001.

[75] L. Ouyang, R. Yao, Y. Zhao, W. Sun, Effect of bioink properties on printability and cell viability for 3D bioplotting of embryonic stem cells, Biofabrication. 8 (2016) 035020. doi:10.1088/1758-5090/8/3/035020.

[76] K. Hölzl, S. Lin, L. Tytgat, S. Van Vlierberghe, L. Gu, A. Ovsianikov, Bioink properties before, during and after 3D bioprinting, Biofabrication. 8 (2016) 032002. doi:10.1088/1758-5090/8/3/032002.

[77] A.C. Daly, P. Pitacco, J. Nulty, G.M. Cunniffe, D.J. Kelly, 3D printed microchannel networks to direct vascularisation during endochondral bone repair, Biomaterials. 162 (2018) 34–46. doi:10.1016/j.biomaterials.2018.01.057.

[78] F. Luo, T.-Y. Hou, Z.-H. Zhang, Z. Xie, X.-H. Wu, J.-Z. Xu, Effects of Initial Cell Density and Hydrodynamic Culture on Osteogenic Activity of Tissue-Engineered Bone Grafts, PLoS One. 8 (2013) e53697. doi:10.1371/journal.pone.0053697.

[79] I. Noshadi, S. Hong, K.E. Sullivan, E. Shirzaei Sani, R. Portillo-Lara, A. Tamayol, S.R. Shin, A.E. Gao, W.L. Stoppel, L.D. Black III, A. Khademhosseini, N. Annabi, In vitro and in vivo analysis of visible light crosslinkable gelatin methacryloyl (GelMA) hydrogels, Biomater. Sci. 5 (2017) 2093–2105. doi:10.1039/C7BM00110J.

[80] K. Nair, M. Gandhi, S. Khalil, K.C. Yan, M. Marcolongo, K. Barbee, W. Sun, Characterization of cell viability during bioprinting processes, Biotechnol. J. 4 (2009) 1168–1177. doi:10.1002/biot.200900004.

[81] A. Blaeser, D.F. Duarte Campos, U. Puster, W. Richtering, M.M. Stevens, H. Fischer, Controlling Shear Stress in 3D Bioprinting is a Key Factor to Balance Printing Resolution and Stem Cell Integrity, Adv. Healthc. Mater. 5 (2016) 326–333. doi:10.1002/adhm.201500677.

[82] M. LI, X. TIAN, J.A. KOZINSKI, X. CHEN, D.K. HWANG, MODELING MECHANICAL CELL DAMAGE IN THE BIOPRINTING PROCESS EMPLOYING A CONICAL NEEDLE, J. Mech. Med. Biol. 15 (2015) 1550073. doi:10.1142/S0219519415500736.

[83] W. Liu, M.A. Heinrich, Y. Zhou, A. Akpek, N. Hu, X. Liu, X. Guan, Z. Zhong, X. Jin, A. Khademhosseini, Y.S. Zhang, Extrusion Bioprinting of Shear-Thinning Gelatin Methacryloyl Bioinks, Adv. Healthc. Mater. 6 (2017) 1601451. doi:10.1002/adhm.201601451.

[84] B.A. Aguado, W. Mulyasasmita, J. Su, K.J. Lampe, S.C. Heilshorn, Improving Viability of Stem Cells During Syringe Needle Flow Through the Design of Hydrogel Cell Carriers, Tissue Eng. Part A. 18 (2012) 806–815. doi:10.1089/ten.tea.2011.0391.

[85] K.S. Lim, B.S. Schon, N. V. Mekhileri, G.C.J. Brown, C.M. Chia, S. Prabakar, G.J. Hooper, T.B.F. Woodfield, New Visible-Light Photoinitiating System for Improved Print Fidelity in Gelatin-Based Bioinks, ACS Biomater. Sci. Eng. 2 (2016) 1752–1762. doi:10.1021/acsbiomaterials.6b00149.

[86] J.W. Nichol, S.T. Koshy, H. Bae, C.M. Hwang, S. Yamanlar, A. Khademhosseini, Cell-laden microengineered gelatin methacrylate hydrogels, Biomaterials. 31 (2010) 5536–5544. doi:10.1016/j.biomaterials.2010.03.064.

[87] T. Hirsch, T. Rothoeft, N. Teig, J.W. Bauer, G. Pellegrini, L. De Rosa, D. Scaglione, J. Reichelt, A. Klausegger, D. Kneisz, O. Romano, A. Secone Seconetti, R. Contin, E. Enzo, I. Jurman, S. Carulli, F. Jacobsen, T. Luecke, M. Lehnhardt, M. Fischer, M. Kueckelhaus, D. Quaglino, M. Morgante, S. Bicciato, S. Bondanza, M. De Luca, Regeneration of the entire human epidermis using transgenic stem cells, Nature. 551 (2017) 327–332. doi:10.1038/nature24487.

[88] A.J. Engler, S. Sen, H.L. Sweeney, D.E. Discher, Matrix Elasticity Directs Stem Cell Lineage Specification, Cell. 126 (2006) 677–689. doi:10.1016/j.cell.2006.06.044.

[89] C.M.F. Potter, K.H. Lao, L. Zeng, Q. Xu, Role of Biomechanical Forces in Stem Cell Vascular Lineage Differentiation, Arterioscler. Thromb. Vasc. Biol. 34 (2014) 2184–2190. doi:10.1161/ATVBAHA.114.303423.

[90] P. Bianco, Stem cells and bone: A historical perspective, Bone. 70 (2015) 2–9. doi:10.1016/j.bone.2014.08.011.

[91] P. Bianco, P.G. Robey, Stem cells in tissue engineering, Nature. 414 (2001) 118–121. doi:10.1038/35102181.

[92] R.C. Riddle, A.F. Taylor, D.C. Genetos, H.J. Donahue, MAP kinase and calcium signaling mediate fluid flow-induced human mesenchymal stem cell proliferation, Am. J. Physiol. Physiol. 290 (2006) C776–C784. doi:10.1152/ajpcell.00082.2005.

[93] L. Ouyang, R. Yao, S. Mao, X. Chen, J. Na, W. Sun, Three-dimensional bioprinting of embryonic stem cells directs highly uniform embryoid body formation, Biofabrication. 7 (2015) 044101. doi:10.1088/1758-5090/7/4/044101.

[94] A. Faulkner-Jones, C. Fyfe, D.-J. Cornelissen, J. Gardner, J. King, A. Courtney, W. Shu, Bioprinting of human pluripotent stem cells and their directed differentiation into hepatocyte-like cells for the generation of mini-livers in 3D, Biofabrication. 7 (2015) 044102. doi:10.1088/1758-5090/7/4/044102.

[95] M. Costantini, J. Idaszek, K. Szöke, J. Jaroszewicz, M. Dentini, A. Barbetta, J.E. Brinchmann, W. Święszkowski, 3D bioprinting of BM-MSCs-loaded ECM biomimetic hydrogels for *in vitro* neocartilage formation, Biofabrication. 8 (2016) 035002. doi:10.1088/1758-5090/8/3/035002.

[96] M.A. Yassin, K.N. Leknes, T.O. Pedersen, Z. Xing, Y. Sun, S.A. Lie, A. Finne-Wistrand, K. Mustafa, Cell seeding density is a critical determinant for copolymer scaffolds-induced bone regeneration, J. Biomed. Mater. Res. Part A. 103 (2015) 3649–3658. doi:10.1002/jbm.a.35505.

[97] R.S. Tare, J. Kanczler, A. Aarvold, A.M.H. Jones, D.G. Dunlop, R.O.C. Oreffo, Skeletal stem cells and bone regeneration: Translational strategies from bench to clinic, Proc. Inst. Mech. Eng. Part H J. Eng. Med. 224 (2010) 1455–1470. doi:10.1243/09544119JEIM750.

[98] Y. Lai, Y. Li, H. Cao, J. Long, X. Wang, L. Li, C. Li, Q. Jia, B. Teng, T. Tang, J. Peng, D. Eglin, M. Alini, D.W. Grijpma, G. Richards, L. Qin, Osteogenic magnesium incorporated into PLGA/TCP porous scaffold by 3D printing for repairing challenging bone defect, Biomaterials. 197 (2019) 207–219. doi:10.1016/j.biomaterials.2019.01.013.

[99] D. Liu, J. Fu, H. Fan, D. Li, E. Dong, X. Xiao, L. Wang, Z. Guo, Application of 3D-printed PEEK scapula prosthesis in the treatment of scapular benign fibrous histiocytoma: A case report, J. Bone Oncol. 12 (2018) 78–82. doi:10.1016/j.jbo.2018.07.012.

[100] N. V. Mekhileri, K.S. Lim, G.C.J. Brown, I. Mutreja, B.S. Schon, G.J. Hooper, T.B.F. Woodfield, Automated 3D bioassembly of micro-tissues for biofabrication of hybrid tissue engineered constructs, Biofabrication. 10 (2018) 024103. doi:10.1088/1758-5090/aa9ef1.

[101] A.C. Daly, D.J. Kelly, Biofabrication of spatially organised tissues by directing the growth of cellular spheroids within 3D printed polymeric microchambers, Biomaterials. 197 (2019) 194–206. doi:10.1016/j.biomaterials.2018.12.028.

[102] W. Zhu, X. Qu, J. Zhu, X. Ma, S. Patel, J. Liu, P. Wang, C.S.E. Lai, M. Gou, Y. Xu, K. Zhang, S. Chen, Direct 3D bioprinting of prevascularized tissue constructs with complex microarchitecture, Biomaterials. 124 (2017) 106–115. doi:10.1016/j.biomaterials.2017.01.042.

[103] V. Keriquel, H. Oliveira, M. Rémy, S. Ziane, S. Delmond, B. Rousseau, S. Rey, S. Catros, J. Amédée, F. Guillemot, J.-C. Fricain, In situ printing of mesenchymal stromal cells, by laser-assisted bioprinting, for in vivo bone regeneration applications, Sci. Rep. 7 (2017) 1778. doi:10.1038/s41598-017-01914-x.

[104] X. Cui, D. Dean, Z.M. Ruggeri, T. Boland, Cell damage evaluation of thermal inkjet printed Chinese hamster ovary cells, Biotechnol. Bioeng. 106 (2010) 963–969. doi:10.1002/bit.22762.

[105] D.B. Kolesky, R.L. Truby, A.S. Gladman, T.A. Busbee, K.A. Homan, J.A. Lewis, 3D Bioprinting of Vascularized, Heterogeneous Cell-Laden Tissue Constructs, Adv. Mater. 26 (2014) 3124–3130. doi:10.1002/adma.201305506.

Cell line	Density	Biomaterial	Cell survival		Construct Size	In vivo	Printing	Ref.
hMSCs	*in vitro* 5×10^6 cells/mL	Alginate	d0	89%	10 layers, 1×2cm, 10µm layer thickness	mice, subcutaneous (*in vivo* 1×10^7 cells/mL)	BioScaffolder (SYS+ENG)	[71]
haChs	*in vitro* 3×10^6 cells/mL							
HCECs		Gelatin-Alginate + sodium citrate	d0	94.6%	8 layers, 30 × 30 × 3.6mm, 0.8mm layer thickness	X	custom-made	[6]
hChs	10^6 cells/mL	Alginate	d1 d7	90– 94% 93.9%	20 layers, 20 × 20 × 2mm, 250 µm pore size, layer thickness 750µm	X	custom-made: multi-head tissue/organ building system (MtoBS)	[56]
MG63			d1 d7	90–94% 95.6%				
MC3T3-E1	$2.3\text{-}2.8 \times 10^5$ /mL	Alginate	d1	84%	27 × 27 × 4.5 mm t) pore size 488µm layer thickness Alginate: 466µm; PCL: 437µm	X	custom-made (melt pot and dispensing system)	[57]
hMSCs and gMSCs cells	$5\text{-}10 \times 10^6$ cells/mL	Alginate	porous constructs d3 d7 solid graft d3 d7	 85% 68% 41%	10 × 10 × 1mm pores 0.8 mm (solid) and 2mm (porous) and a fibre height of 100 µm	mice, subcutaneous	BioScaffolder (SYS+ENG)	[40]
hASCs, hTMSCs and L6	$1\text{-}5 \times 10^6$ cells/mL	decellularized extracellular matrix (dECM)	d1 d7-d14	95% 90%	*hdECM 10 × 10 × 1mm cdECM 6 × 6 × 3mm adECM 10 × 10 × 4mm	X	custom-made: multi-head tissue/organ building system (MtoBS)	[50]
hESC-derived HLCs	1×10^7 cells/mL	Alginate	*hESCs 86%		40 layers (13mm)	X	custom-made nanolitre dispensing system	[94]
hiPSC-derived HLCs			hiPSCs 63%					
hMSCs, hNDFs and HUVECs	1×10^7 cells/mL	Gelatin–Fibrinogen (hMSCs and hNDFs) Pluronic F127 (HUVECs)	d0	95% (gelatin processing temperature 95°C)	725 × 650 × 125 mm, 100-410µm diameter nozzle	X	custom-made (4 independent printheads)	[67]
HNDFs 10T1 / 2s HUVEC	2×10^6 cells/mL	PLURONIC F127, Gelatin Methacrylate (GelMA)	d0 d7 d0 d7	HNDFs 70% 81% 10T/12 61% 82%	*10 × 10 mm, 6 layers height	X	custom-made (4 independent printheads)	[105]
hAFSCs,	5×10^6 cells/ml	Gelatin, Hyaluronic Acid, Glycerol, Fibrinogen, Pluronic F127 as sacrificial material	d1	91%	Mandible bone reconstruction 3.6 × 3 × 1.6 cm	Calvarial bone defect 8 mm diameter × 1.2 mm thickness	Integrated Tissue–Organ Printer (ITOP)	[1]
reChs,	40×10^6 cells/ml		d1	91%	Ear Cartilage 3.2 × 1.6 × 0.9 cm			
C2C12	3×10^6 cells/ml		d1	97%	Skeletal muscle 15 × 5 × 1 mm			
HepG2	1.5×10^6 cells/mL	Gelatin Methacrylamide	d0	> 97%	13 × 13 × 1-3 mm thickness, 150-200 µm layer thickness, and fibres spacing of 350 and 550 µm	X	Bioplotter Envisiontec, GmbH	[64]

BMSCs	2.5×10^5 cells/mL	Lutrol F127	*Lutrol F 127 d1 25% d3 5% d7 2%	20 × 20mm with spacing between fibres of 300 µm and 150 µm layer thickness	X	Bioplotter Envisiontec, GmbH	[33]
		Matrigel	Matrigel d1 95%, d3 90% d7 98%				
		Alginate	Alginate d1 90% d3 90% d7 97%				
		Methylcellulose	Methylcellulose d1 d3 d7				
		Agarose	Agarose d1 90% d3 70% d7 75%				